

Potential for permanent CO₂ sequestration in depleted volcanic reservoirs in the offshore Campos basin, Brazil

Germano Mário Silva Ramos*, José Antonio Barbosa, Araly Fabiana Lima de Araújo, Osvaldo José Correia Filho, Carla Joana Santos Barreto, Jefferson Tavares Cruz Oliveira, Roberta Samico de Medeiros

GEOQUANTT Laboratory, Department of Geology, Universidade Federal de Pernambuco, Cidade Universitária, Av. da Arquitetura s/n, Recife 50740-550, Brazil

ARTICLE INFO

Keywords:

Geological sequestration of CO₂
CO₂ mineralization mechanisms
Offshore CCS
Pre-salt CO₂ content
Reservoir modeling

ABSTRACT

The pre-salt oil and gas production in Brazil faces a significant challenge due to the high CO₂ content in these reservoirs. Approximately 600,000 t of CO₂ are reinjected monthly in the reservoirs, but the increased production of CO₂ will demand alternatives for sequestration. Experiments and pilot projects have demonstrated the viability of CO₂ sequestration through the mineralization method in basaltic rocks. Here, we present a study aimed at demonstrating the feasibility of using the volcanic rocks of the Cabiúnas Formation, located at the base of the pre-salt section in shallow waters of the Campos Basin, for CCS projects. We used legacy data to determine the regional characteristics and porosity distribution of the volcanic sequence to assess the feasibility of geological sequestration in this region. Our estimates demonstrated that the Cabiúnas flood basalts have a good to excellent storage capacity. The modeling of a 31 km² hypothetical reservoir with a thickness of 300 m in the upper part of the sequence above the Badejo Field revealed a storage estimate of 16–47 Mt. The technical aspects discussed in this study provide valuable insights that can help with the development of future CCS projects in the volcanic rocks of this petroleum province.

1. Introduction

According to the IPCC Special Report for policymakers (2018), the global mean surface temperature between 2006 and 2015 was approximately 0.78 °C greater than the average temperature between 1850 and 1900. The report also stated that both past and present anthropogenic emissions are driving global warming at a rate of approximately 0.2 °C per decade. This report has prompted a series of discussions between governments and global oil and gas industry aimed at adopting several initiatives and policies that focus on the reduction of anthropogenic CO₂ emissions. In particular, the industry must address the destination of the hundreds of gigatons of CO₂ emissions that have entered the atmosphere at an increasing pace in the past few decades (Martin-Roberts et al., 2021). The reduction of emissions can be achieved through the reduction of fossil fuel consumption (Bataille et al., 2020; Fuss et al., 2020) and the capture and sequestration (CCS) of the significant amounts of CO₂ produced by industrial processes; this includes the capture and utilization of CO₂ (CCUS) in gas injection projects in oil reservoirs, which is used to increase the recovery factor (Moghanloo et al., 2017;

Sampaio et al., 2020). The injection of CO₂ in geological media is the most important method of artificial sequestration (Leung et al., 2014), and involves the injection of CO₂ diluted in water or in a supercritical state into saline aquifers, artificial salt caverns, coal deposits, or volcanic mafic rocks (Leung et al., 2014; Ajayi et al., 2019; Kelemen et al., 2019, 2020; Snæbjörnsdóttir et al., 2020; Hong et al., 2022).

Ringrose and Meckel (2019) state that, to cope with the global demand for the IPCC 2 °C scenario, CCS should support approximately 13% of total cumulative emissions reductions (~120 gigatons) through 2050. For nations with large-scale emissions, offshore geologic sequestration would be the most attractive and effective strategy due to its reservoir quality, safety, and cost-effectiveness (Ringrose and Meckel, 2019). However, to meet the modest demands laid out by world governments, it would be necessary to construct between 10,000 to 14,000 CO₂ injection wells globally by 2050. This suggests that Brazil, an emerging player in oil and gas with a large CO₂ footprint, must look at all alternatives available for carbon sequestration (conventional reservoirs, artificial salt caves, CCUS reinjection, and subsurface mineralization). Previous works have already highlighted the potential for CO₂

* Corresponding author.

E-mail address: germano.mario@ufpe.br (G.M. Silva Ramos).

sequestration in the oil fields of the Campos Basin, specifically with respect to the siliciclastic reservoirs, which have sequestration capacities of approximately 950 Mt (Rockett et al., 2013).

Some critical aspects of CCS projects include the costs involved in capture and injection operations, transportation, the geology of the site project, and the safety issues associated with the eventual leakage of CO₂ for long periods after sequestration (Anderson, 2017; Mechler et al., 2017; Alcalde et al., 2018; Schmelz et al., 2020; Gholami et al., 2021). The associated costs of CCS projects include the intrinsic technologies and capacity necessary to capture the CO₂ in the different industrial processes responsible for producing most of the gasses (e.g., oil refining, biofuel production, and the cement industries), transportation options,

the localization of viable storage sites, and the availability of previous infrastructure, such as pipelines or injection wells (Rubin et al., 2013, 2015; Grusson et al., 2015; Cao et al., 2020; Smith et al., 2021). Safety issues include the eventual leakage of CO₂, the displacement of brine through shallow aquifers, and increased seismicity (Damen et al., 2006; Amonette et al., 2014; Matter et al., 2014; Vilarrasa and Carrera, 2015; Fawad and Mondol, 2022).

In this context, Brazilian authorities expect CO₂ emissions generated by the oil and gas production in the pre-salt province, comprised of the Santos and Campos basins in southeastern Brazil (Fig. 1), to increase significantly in the coming decades to tens of millions of metric tons per year (Godoi et al., 2021) due to the ramp-up in production of these

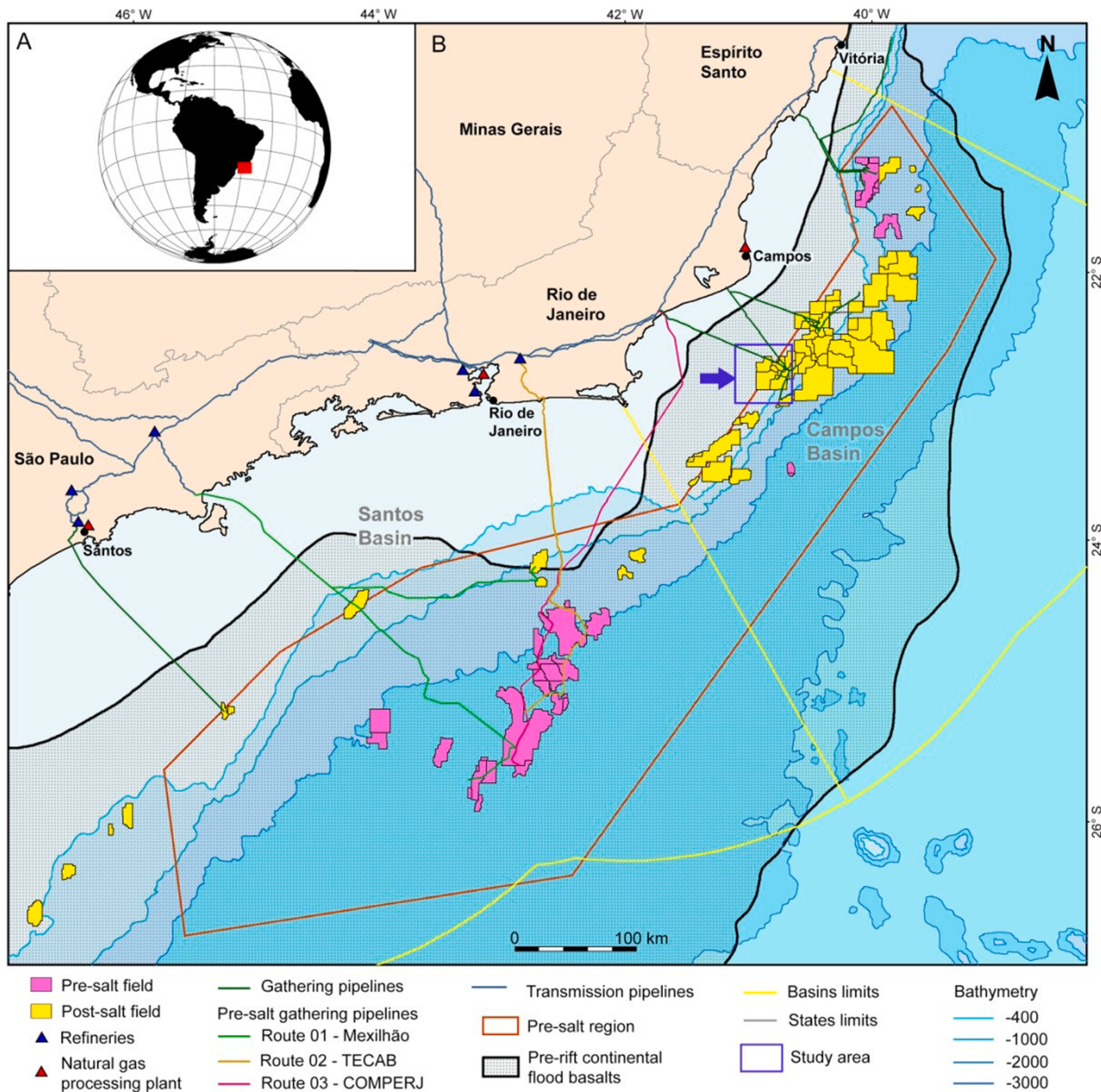


Fig. 1. (A) Location of the pre-salt petroleum province in southeastern Brazil (red polygon). (B) distribution of production oil and gas fields in the Santos and Campos Basin (ANP, 2022). The primary infrastructure, including pipelines, refineries, and natural gas processing plants, are presented (EPE, 2020). The blue arrow indicates the location of the study area. The gray-hatched zone (black polygon) delineates the area covered by continental flood basalts (Stica et al., 2014).

reserves (Fig. 2A and 2B), which possess exceptionally high contents of CO₂ (Fig. 1) (Beltrão et al., 2009; Pizarro e Branco, 2012; Viglio et al., 2017; Lima et al., 2020; Sampaio et al., 2020). In 2021 Brazil produced an average of 2.9 million b/d and 136 million m³/d of oil and gas, respectively, and it is expected that production will reach 5.2 million b/d of oil and 1.6 million boe/d of natural gas in 2030 (National Company for Energy Studies [EPE], 2021). Indeed, the Campos Basin

possesses an average CO₂ concentration of 0.5%, with values of up to 20% near its boundary with the Santos Basin (Fig. 2C) (d'Almeida et al., 2018). Most wells drilled into the pre-salt interval of the Santos Basin report CO₂ concentrations of 5%, with some wells reporting concentrations of up to 50–80% (Fig. 2C) (Santos Neto et al., 2012; Matias et al., 2015; Cornelius, 2021; de Freitas et al., 2022). The higher concentrations of CO₂ in Santos Basin are located in its southeastern,

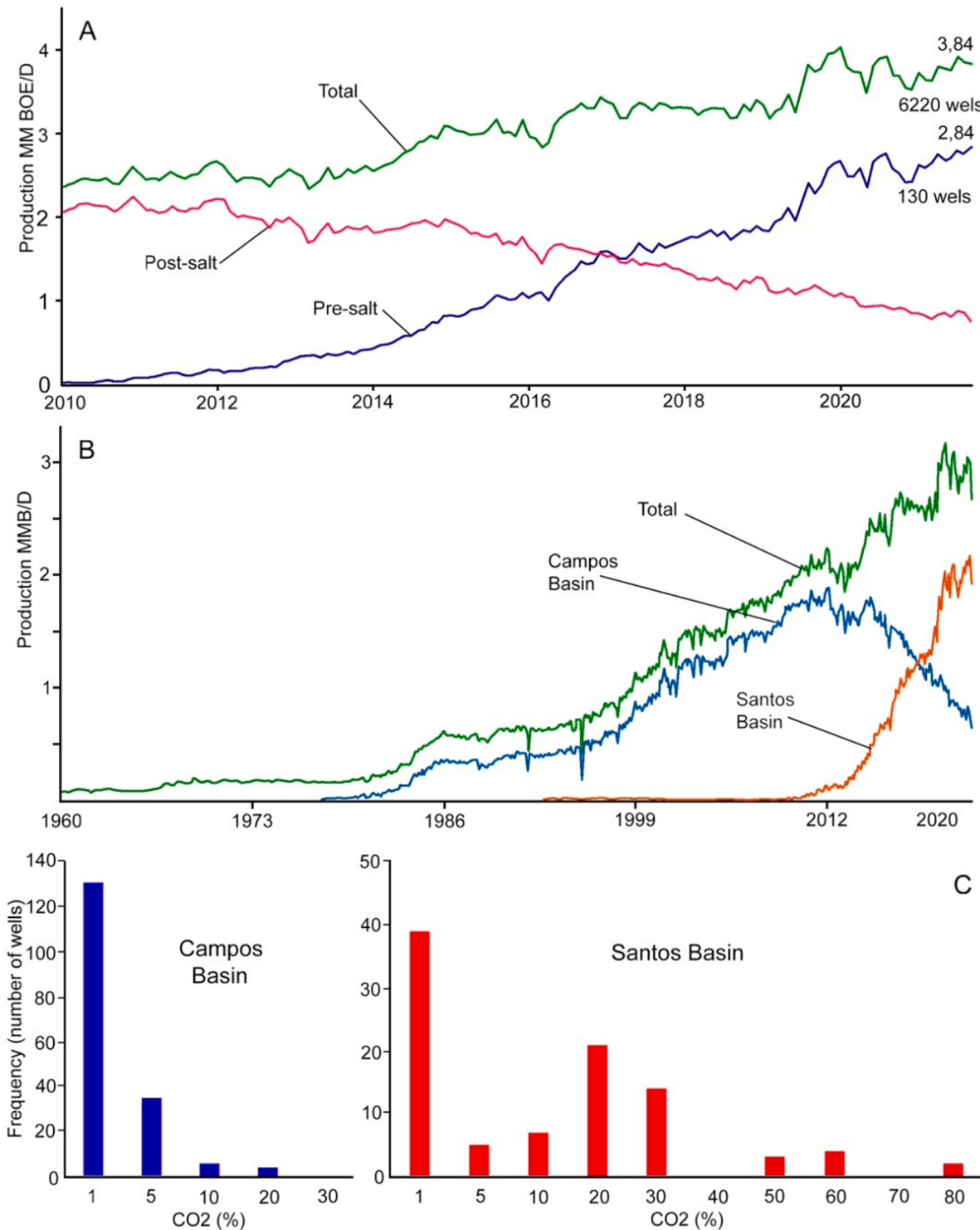


Fig. 2. (A) The contribution of post-salt and pre-salt fields to total Brazil's hydrocarbon production in the last decade (MM BOE/D - million barrels of oil equivalent per day). (B) The historical contribution of the Santos and Campos basins to Brazil's hydrocarbon production (MMB/D Million barrels per day). It highlights the rapid decline of the Campos fields as well as the increase in Santos Basin production due to the development of operations in the pre-salt interval (adapted from ANP, 2021). (C) A histogram depicting the%CO₂ content in wells drilled in the pre-salt reservoirs (adapted from Almeida et al., 2018).

ultra-deepwater regions. The CO₂ present in the natural gas produced from the Lula field, the first field to extract natural gas from the pre-salt interval, varies between 8 and 25%, while the natural gas produced from the Iracema accumulation (part of the Lula field; Fig. 2C) contains approximately 1% CO₂ (EPE, 2019, 2020). The origin of CO₂ is likely associated with mantle contamination (Gamboa et al., 2019). Recent data showed that the total CO₂ production from the Brazilian pre-salt intervals reached 630,000 t in July 2021, equivalent to 7 Mt of CO₂ per year (SandP Global, 2021).

Fig. 2A and B show the historical contribution of the Santos and Campos basins to Brazilian hydrocarbon production. The impact of production in the 1980s and the 1990s came from the post-salt reservoirs of the Campos Basin (mainly Cenozoic turbidites) (Guardado et al., 1990; Bruhn et al., 2003), while a majority of the increased production in the last decade came from pre-salt fields found in the Santos Basin (Fig. 2) (National Agency for Petroleum, Natural Gas, and Biofuels [ANP], 2019; 2021). The investment and development of the pre-salt interval in the deep waters of the Campos and Santos Basins continue to evolve rapidly, and current predictions suggest a production of 4 MMboe/d around 2030 (EPE, 2020). The number of wells operating in the post-salt compared to the pre-salt interval (Fig. 2A), highlight the greater productivity of the pre-salt reservoirs. However, the CO₂ content in the hydrocarbon reserves found in pre-salt wells is also considerably higher (Fig. 2C) (ANP, 2021).

One of the CCUS operations in this area is the CO₂ water-alternating-gas (WAG) injection, in which most of the CO₂ produced in the pre-salt fields is reinjected into the reservoirs to increase their recovery factor (IOR/EOR) (Pizarro and Branco, 2012; Lima et al., 2020; Sampaio et al., 2020; Godoi et al., 2021; Pereira et al., 2021). Most of the natural gas that is not transported to the continent and not used in offshore installations is also reinjected into the reservoirs (EPE 2020). However, it is expected that pre-salt production will generate between 200 and 300 million tons of CO₂ in the next three decades, and the capacity of reservoirs to receive the CO₂ may be reduced due to the growing risk of formation damage (e.g., negative influences on the temperature, permeability, and geomechanics of the rocks) (Drexler et al., 2019; Godoi et al., 2021) as well as damage to the equipment caused by CO₂-related problems (e.g., accelerated failures, increasing manutention costs) (Beltrão et al., 2009). Another technology that has been proposed to address the CO₂ sequestration is the utilization of artificial salt caverns in the deep-water evaporites deposits that cover the reservoirs in the distal domains of the Santos and Campos basin (Fig. 1) (Costa et al., 2019; Goulart et al., 2020).

The safety and the effectiveness of keeping CO₂ sequestered in geological media during and after the injection project are the primary issues that affect the cost of the operation (Friedmann et al., 2006; Stenhouse et al., 2009; Aydin et al., 2010; Ajayi et al., 2019; Cao et al., 2020). In some cases, the monitoring required could represent up to >50% of the project costs (Takagi et al., 2013). Injection in saline aquifers, depleted oil and gas reservoirs, and salt caves raise the possibility of long-term leakage due to the mobility of CO₂, seal damage, and well failures (Bérest and Brouard, 2003; Damen et al., 2006; Vilarrasa, 2014; Pawar et al., 2015; Bai et al., 2016; Warren, 2017; Cao et al., 2020; Dinescu et al., 2021; Gholami et al., 2021). Furthermore, the injection of large amounts of CO₂ in offshore areas presents even more challenges due to the logistics involved (Stenhouse et al., 2009; Rubin et al., 2015) as well as the intrinsic characteristics of the reservoir (Takagi et al., 2013; Anderson, 2017; Schmelz et al., 2020). A better understanding of the costs and risks associated with different CCS methods, especially with regard to the various geological uncertainties, is required (Aydin et al., 2010; Vilarrasa and Carrera, 2015; Aminu et al., 2017; Alcalde et al., 2018; Larkin et al., 2019; Cao et al., 2020; Schmelz et al., 2020). The sequestration of CO₂ from pre-salt production will likely demand multiple simultaneous CCS methods focused on offshore solutions due to the remote location of the production infrastructure (Figs. 1 and 2).

The sequestration of CO₂ via mineral carbonation is an emerging

technology based on the injection of supercritical or diluted CO₂ into basaltic rocks (Gislason et al., 2014; Matter et al., 2014; Gunnarsson et al., 2018). This method aims to trap free CO₂ molecules within solid composites; specifically, carbonate minerals (CaCO₃, MgCO₃, FeCO₃) (Kelemen et al., 2019; Pogge et al., 2019). The CO₂ injection produces carbonic acid, which reacts with mafic rock, and induces the liberation of cations (e.g., Ca²⁺, Mg²⁺, and Fe²⁺) from the dissolution of Ca- and Mg-bearing silicate and alumino-silicate minerals like olivine, plagioclase, and diopside (Gislason et al., 2014; Kelemen et al., 2020; Snæbjörnsdóttir et al., 2020; Ali et al., 2022; Raza et al., 2022). The reactions are mediated by the partial CO₂ pressure, temperature, and pH of the solution.

The criteria used to identify appropriate sites for mineralization-based CCS projects in volcanic mafic rocks include alkaline water (pH > 7), temperatures ranging from 50 to 250 °C, and pressure ranging from 0.6 to 50 MPa (Kelemen et al., 2020; Raza et al., 2022); these represent the key parameters of the chemical reactions. The influence of other factors, such as injectivity and specific mineral wettability in carbonate mineral formations, is still not completely understood. However, the success of CO₂ sequestration through injection in mafic rocks represents the potential to remove billions of tons of CO₂ per year (Gislason et al., 2014; Snæbjörnsdóttir et al., 2020; Tutolo et al., 2021; Raza et al., 2022).

This study focuses on the Neocomian flood basalt sequence of the Cabiúnas Formation (Sin-rift phase) that covers the Precambrian basement of the Campos Basin, southeastern Brazil (Mizusaki et al., 1988; Guardado et al., 1990; Oreiro, 2006). During the 1980s and the 1990s, the oil-bearing fractured basalts of the Cabiúnas Formation found in the Badejo Field were developed as unconventional reservoirs (Bruhn et al., 2003; Lobo et al., 2007) (Fig. 2). Based on the availability of legacy data (2D and 3D seismic surveys, potential field data, and well data), physical infrastructure, and the proximity of the pre-salt fields, we report an evaluation of the potential of establishing large offshore CO₂ sequestration hubs in these basaltic deposits (Fig. 2). This article aims to investigate the feasibility of CO₂ sequestration in the Cabiúnas basaltic rocks based on their theoretical suitability concerning the mineralization trapping process (Raza et al., 2022) and their capacity in terms of storage volume. We have considered the method based on the injection of water-charged (dissolved) CO₂ (Snæbjörnsdóttir et al., 2020) to estimate the storage volume, however the injection of supercritical CO₂ could also be used due to the characteristics of the sedimentary succession.

Injection of water-dissolved (CarbFix pilot) and supercritical (Wallula pilot) CO₂ was tested for the geological sequestration of CO₂ in basaltic rocks (McGrail et al., 2014; Snæbjörnsdóttir et al., 2018). The feasibility of the reactive effects and mineral formation with the CO₂ trapping has been proved for both alternatives (Macgrail et al., 2009; Kelemen et al., 2019; Raza et al., 2020; Tutolo et al., 2021). Due to the buoyancy of the free phase plume formed by the injection of supercritical CO₂, the project needs to consider a seal cap rock, which is not the case for the water-dissolved injection method (Snæbjörnsdóttir et al., 2020; Tutolo et al., 2021). In the case presented, seal rocks occur over the basaltic succession, which also allow the injection of supercritical CO₂ as another option in terms of method. The main advantage of the supercritical injection is the larger amount of gas that could be injected. Tutolo et al. (2021) pointed out some advantages of injecting supercritical CO₂ in basaltic rocks, markedly the per-well capacity of injection, which will imply a lesser number of wells needed to accomplish large sequestration volumes. However, as discussed by Snæbjörnsdóttir et al. (2020), available water is not a limitation in offshore projects. The energy-consuming process of the water-gas mixture before injection could be less costly than the need to execute WAG (water-gas alternating injection) operations which could be needed to increase the supercritical injection, as discussed by Tutolo et al. (2021). The most crucial consideration for adopting the water-dissolved method is that the free-phase injection will increase the costs of monitoring. The lack of

reliable data about the results of long-term injection of large amounts of CO₂ in both forms will lead to the initial adoption of more conservative options initially, and possibly the water-dissolved form could be tested with fewer risks.

There are two main advantages to utilizing these basaltic rocks: 1)

the proximity between the CO₂ emission sources (the pre-salt production facilities) and the basaltic reservoirs (Figs. 1 and 3) and 2) the reliable trapping mechanism, ensured by the mineralization process, and the overlying seal rocks (shales, carbonates, and evaporites from the rift and transitional phases), which will also allow the injection of supercritical

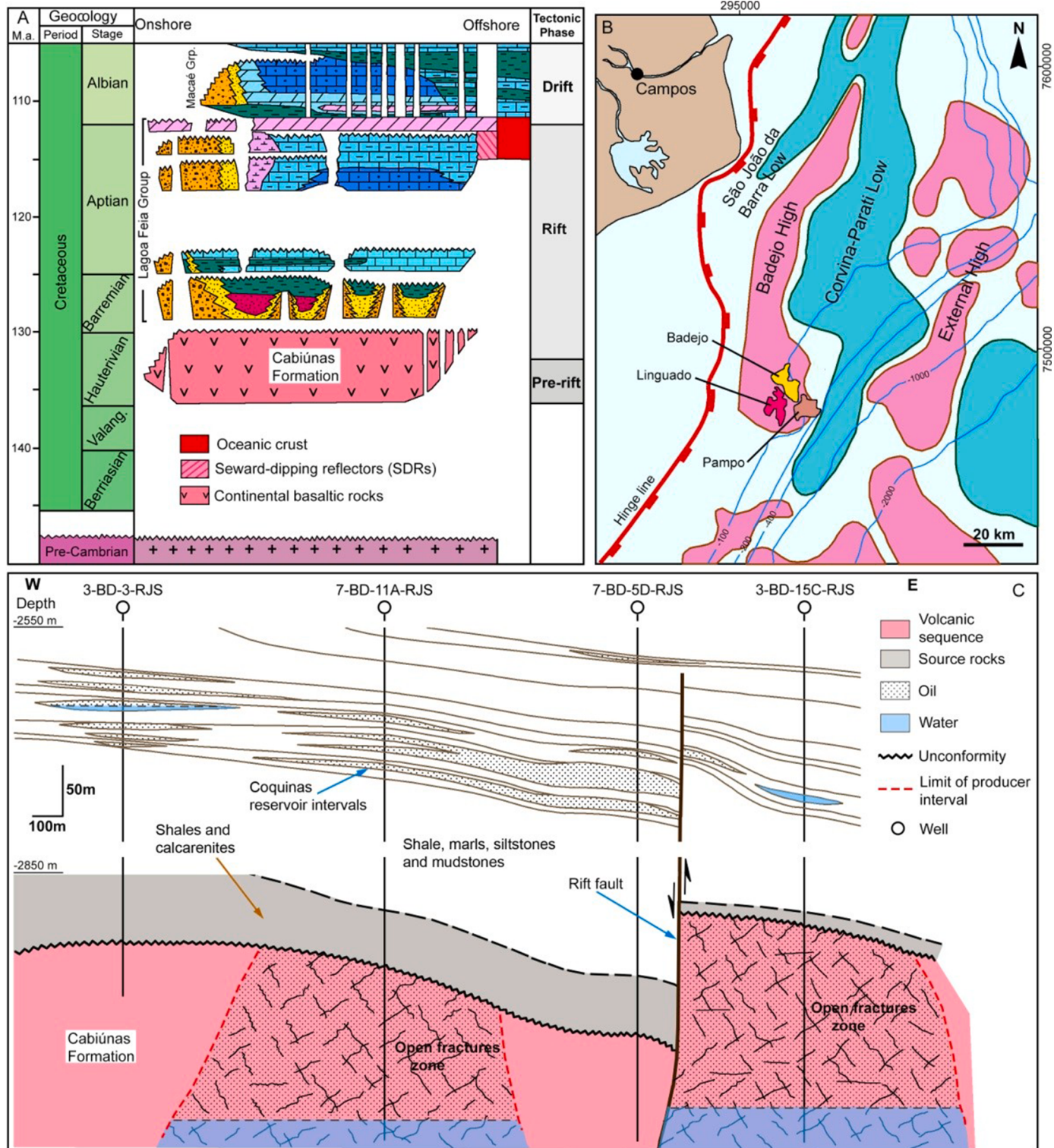


Fig. 3. (A) A simplified stratigraphic column of the Campos Basin that shows the Hauterivian-Albian succession (adapted from Stica et al., 2014). (B) The regional tectonic compartmentalization of the Campos Basin, highlighting regional highs and the location of the Badejo-Linguado-Pampo fields where oil was produced from the volcanic sequence of Cabiúnas Formation (de Castro and Picolini, 2016). (C) A schematic geological section across Badejo Field showing how the hydrocarbon reservoirs were accumulated in the carbonate rocks (Lagoa Feia Grp.) and in the underlying fractured basaltic rocks (modified from Guardado et al., 1990).

CO_2 .

Our analysis showed that this alternative is technically feasible and that the basaltic rocks could store vast quantities of CO_2 , and helps the industry to cope with CO_2 issues in the coming decades.

2. Geological setting

The petroleum system of Campos Basin is comprised of good quality source rocks (shales) from the rift phase Lagoa Feia Group (freshwater lacustrine to brackish lacustrine facies from the Coqueiros and Atafona formations), which represent the primary oil-generating intervals (Guardado et al., 2000; Bruhn et al., 2003; de Lima et al., 2022) (Fig. 3). Reservoirs are represented by fractured basalts (Neocomian), Coquinas (Barremian), Early to Middle Albian calcarenites and calcirudites (Fig. 3A), and Late Albian to Early Miocene turbidites (Guardado et al., 1990; Rosa and Vicentelli, 2017). The study area also includes the geological trends formed by the Linguado, Badejo, and Pampo fields, located in the northwestern part of the Campos Basin (Figs. 1 and 3), between 100 and 300 m water depth (Fig. 3B). Wells drilled to explore the carbonate and siliciclastic formations below the salt layer in this region also found oil in the fractured basalts deposited over the Precambrian basement (Guardado et al., 1990, 2000; Mohriak et al., 1990; Bruhn et al., 2003; Ren et al., 2020). The rift phase of the Campos Basin also involved the development of normal (synthetic and antithetic) and transcurrent faults, which controlled the formation of grabens and horsts along the proximal and distal regions of the basin (Guardado et al., 1990; Milani and Thomaz Filho, 2000; de Castro and Picolini, 2016). Siliciclastic and shallow carbonates formations were deposited during the transitional phase, followed by Aptian evaporites, while the drift phase included the deposition of carbonates and siliciclastics from the Albian to the Quaternary (Bruhn et al., 2003; de Lima et al., 2022).

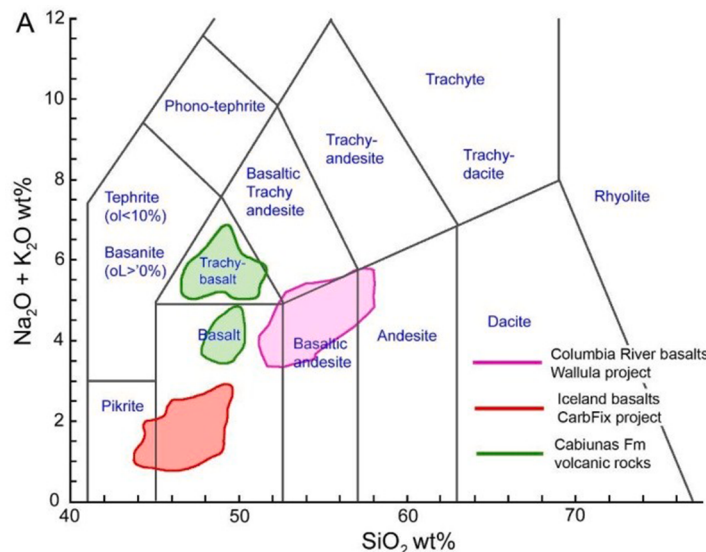
The evaporite interval in the continental platform in this region (Fig. 3B) is thinner than in the distal parts of the Campos and Santos basins. Here, the sedimentary deposition and the petroleum system were primarily controlled by a series of elongated paleo-highs and lows that trend mainly NNE–SSW (Fig. 3). The main accumulations of oil and gas found in pre-salt deposits in the Badejo, Linguado, and Pampo fields (siliciclastics and carbonates) were formed through the fault-controlled migration of hydrocarbons from the source rocks of the rift-phase (Fig. 3C). Reservoirs formed over horsts in the Badejo High (Fig. 3B), including the oil-bearing Hauterivian flood basalts of the Cabiúnas

Formation in the Badejo Field (de Castro, 2006; de Castro and Picolini, 2016; Mizuno et al., 2018). The Cabiúnas Formation is comprised of interbedded lava flows, sandstones, breccias, and pyroclastic flow units (Mizusaki et al., 1988). The migration and accumulation of oil to the Cabiúnas unit occurred due to the lateral contact between source rocks and basaltic rocks and were primarily controlled by rift faults (Fig. 3C).

2.1. Reservoir characteristics

The igneous rocks of the Cabiúnas Formation are comprised of a poorly differentiated transitional to sub-alkaline sequence that is continental in origin (Mizusaki, 1986; Mizusaki et al., 1988; Marins et al., 2022). Mizusaki et al. (1988) suggested that the sequence also includes successive cycles of interbedded volcaniclastic and sedimentary rocks (sandstones containing clasts of volcanic rocks) (Fig. 4). Each of these cycles was subdivided into 1) lava flows, which exhibit different textures (vitreous basalts, microcrystalline basalts, and vesicular basalts) due to the effect of cooling and their interaction with surface fluids; 2) pyroclastic (hydrovolcanic) breccias; 3) tuffs, commonly altered due to subaerial exposure; and 4) sandstones containing volcanic clasts (Fig. 4B) (Guardado et al., 1990). They argued that this cycle is incomplete in most wells, with the tuffs and sedimentary rocks missing (Fig. 4) (Mizusaki et al., 1988; Guardado et al., 1990; Marins et al., 2022). The individual basalt flows cover large areas, tend to have planar morphologies, and have thicknesses between 3 and 4 m that eventually reach up to 10 m (Mizusaki et al., 1988). Other than the basalts, some diabase and rocks with trachytic textures were found, but their relative volume is very small (Mizusaki, 1986; Mizusaki et al., 1988). Marins et al. (2022) have also described the peperites and the complex interaction between volcanic and sedimentary deposits in this region.

The depth of the Cabiúnas Formation ranges from 2800–3,000 m, but no wells have reached the continental basement below this unit, and its thickness remains unknown. Mizusaki et al. (1988) also identified a regional system that involved subaerial and subaqueous volcanism that described the distribution of volcanic, pyroclastic, and volcaniclastic rocks. Marins et al. (2022) also recognized the continental and subaqueous influences on deposition based on microfossils. The distribution of depositional environments proposed by Mizusaki et al. (1988) is shown in Fig. 5A and is represented by zones named A to E going from north to south, which cover the three fields studied (Fig. 5). Zone A is characterized by successions formed by basalts/auto-breccias,



Lithofacies	Porosity type				
	Macro-fracture	Micro-fracture	Vesicle	Micro-porosity	Reservoir quality
Sandstone				█	Poor
Pyroclastic			█		Poor
Breccia	█				Fair
Vesicular basalt		█			Good
Microcrystalline basalt	█				Good
Vitreous basalt	█				Fair

Fig. 4. (A) Classification of the basaltic rocks of the Cabiúnas Formation as well as the rocks used in the injection projects based on the relationship between their silica and alkali contents (TAS Diagram) (Mizusaki, 1986; Mizusaki et al., 1988; Alfredsson et al., 2013; Fox, 2022). (B) General correlation between the lithofacies in a cycle formed by volcanic, pyroclastic, and sedimentary rocks of the Cabiúnas Formation as well as their reservoir quality (Modified from Guardado et al., 1990).

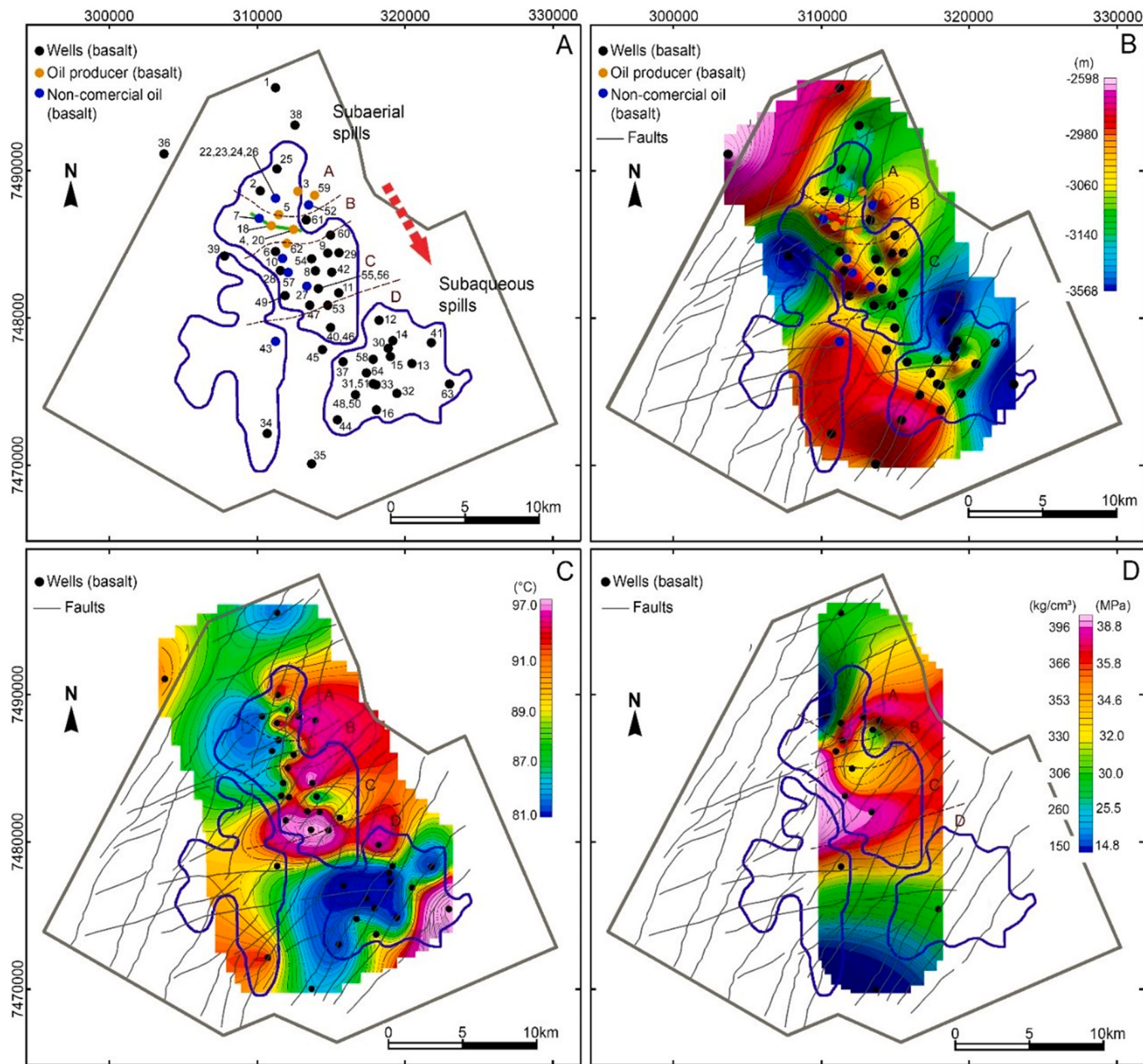


Fig. 5. (A) Outline of the 3D seismic data (PSTM and PSDM volumes) used to study the regional characteristics of the volcanic sequence (Cabiúnas Formation). The locations of the 64 wells used in this study are indicated by black dots. The red arrow highlights the change in the depositional trend (dashed lines) from subaerial (zone A) to subaqueous conditions (zones C and D) that prevailed during the formation of the basaltic and volcanoclastic rocks (Mizusaki, 1986; Mizusaki et al., 1988). (B) A contour map describing the depth to the top of the Cabiúnas formation based on well data (gray thin lines represent regional faults mapped on the seismic data). (C) A map of the interpolated temperature values within the Cabiúnas deposits based on data acquired from the wells. D) A map of the interpolated formation pressure values obtained from tests conducted on the wells. The extent of the Badejo, Linguado, and Pampo fields are shown using blue polygons.

basalts/tuffs, and subaerial conditions (evidenced by oxidation and pedogenetic features). Zone B is characterized by successions formed by basalts/sandstones and basalt/volcaniclastics/hydrovolcanic breccias. Sediments in this zone indicate a coastal environment, with hydrovolcanic breccias also indicating subaqueous volcanism. Zone C is characterized by successions composed of basalts/auto-breccias and basalt/volcaniclastics/hydrovolcanic breccias, with evidence that they were formed in a subaqueous environment. Zone D is also characterized by successions of basalts/tuffs, and there is evidence to suggest that the tuffs formed in this zone were formed subaqueously in a lacustrine environment (Mizusaki, 1986; Mizusaki et al., 1988; Guardado et al., 1990) (Fig. 5A). According to Mizusaki et al. (1988), the lava flows in

the Linguado Field are gray, rarely possess vesicles, and have fewer fractures compared to basalts from the Badejo Field (Fig. 5).

The basalts of the Cabiúnas Formation are aphanitic and can be classified into three groups: 1) hyaline, composed of plagioclase, clinopyroxene, and magnetite; 2) hemicrystalline, composed of plagioclase, clinopyroxene, olivine, and magnetite; and 3) holocrystalline, composed of plagioclase, clinopyroxene, olivine, and magnetite. Volcanic glass is abundant, frequent and rare in hyaline, hemicrystalline, and holocrystalline basalts, respectively. Vesicles are abundant in the hyaline basalts and rare in the other textures. The alteration of these basalts resulted in the formation of smectite and chlorite which are found filling the vesicles and fractures (Mizusaki, 1986; Mizusaki et al.,

1988). Igneous rocks of the Cabiúnas Formation are represented by potassic and sodic trachybasalts, basalts, secondary mugearites, and continental tephrites (Fig. 4A). Of the samples analyzed by Mizusaki (1986), 66% were supersaturated, 24% were lightly sub-saturated with olivine, 5% were sub-saturated with olivine and nepheline, and 5% were sub-saturated with nepheline (Fig. 4A). Fig. 4A shows the comparison between the Cabiúnas basalts properties and other basaltic formations used for CO₂ mineralization projects.

Mizusaki et al. (1988) also suggested that the sedimentary and volcaniclastic rocks did not represent any reservoir potential; this was corroborated by an analysis performed by Marins et al. (2022). The oil production was related to the wells drilled in the Badejo Field (oil; 31° API), and few oil discoveries were made in the basaltic sequence of Linguado Field (oil; 28° API), but they were non-commercial.

According to Bruhn et al. (2003), oil was discovered in the Badejo Field in 1975, and production started in 1981. The estimated volume of original oil in place (OOIP) in the fractured basalts was 45 million barrels. At the end of the 1980s, the field was producing approximately 6800 bbl of oil/day with a cumulative production of 13 million bbl. Two-thirds of the total production came from three wells that drained the fractured basalts of the Badejo Field.

The reservoir zones were represented by intensely fractured rocks with sub-vertical fractures that cut several basaltic flows. These fractures were attributed to a late tectonic event (Mizusaki, 1986). Data obtained from the testing of core samples showed that the matrix porosity of the igneous rocks of the Cabiúnas Formation was dominated by microporosity (<1 μm) and varied between 0.69–7.5%. The higher porosity values were commonly associated with altered rocks. Matrix permeability varied from 0.7 to 1.0 mD (Mizusaki, 1986). Tests performed in core samples by Marins et al. (2022) were consistent with these findings, reporting matrix permeabilities of 0.1–1.0 mD in the volcanic rocks.

Guardado et al. (1990) reported that the crude oil in the Badejo Field primarily occurred in fractures, microfractures, and vesicles. Vertical fractures were found to be abundant in the top and base of each volcanic-sedimentary cycle, and horizontal fractures were common in the central sections of the cycles, which increases the permeability of the rocks. The porosity and permeability of the breccia zones were similarly influenced by fracturing and were increased by acidic injections that dissolved calcite cement. According to Mizusaki (1986), vesicles are common in the upper sections of the lava flows and are filled with calcite, zeolites, and authigenic clay minerals. In core samples taken from the drilled wells, the aperture of the microfractures varied from 10 to 50 μm, and the aperture of vertical to sub-vertical fractures ranged from a few millimeters up to 2 cm. Some fractures were found filled or partially filled with calcite, chlorite, zeolites, iron oxides, and pyrite. Authigenic minerals, listed according to their abundance, are calcite, chlorite, smectite, micro-crystalline quartz, chalcedony, zeolites, and serpentines (Mizusaki, 1986).

Recently, Marins et al. (2022) studied the volcanic and volcaniclastic rocks sampled from the Badejo and Linguado fields, focusing on the characterization of the lithofacies and their reservoir properties. These authors suggested that these volcanic, volcaniclastic, and sedimentary rocks were primarily formed subaerially and divided their occurrence into four units comprised of interbedded volcanic and sedimentary rocks. Units 1 and 3 were dominated by pahoehoe lava flows, while units 2 and 4 were dominated by rubbly pahoehoe lava flows. Subaerial weathering controlled the porosity and permeability of the rocks. Intense alteration led to the infilling of vesicles and fractures with clay minerals as well as the formation of non-reservoir zones. Marins et al. (2022) also reported the secondary filling of fractures and vesicles with quartz, chlorite, magnesian smectite, chlorite/smectite, and calcite, in that order. These authors also suggested that the top of rubbly lava flows exhibited greater porosities. In addition to the occurrence of cooling joints, the authors also recognized the occurrence of tectonic fractures and fault damage zones, as previously reported by Mizusaki (1986) and

Mizusaki et al. (1988). Their analysis of the permeability and porosity of volcanic and sedimentary rocks corroborated the information reported by Mizusaki et al. (1988). Most of the rocks sampled possessed a matrix permeability of <0.1 mD, and some samples of the rubbly lava and the vesicular basalts exhibited permeabilities between 0.1–1.0 mD, with a few rubbly samples reaching up to 10 mD. The porosity of most rocks ranged from 1 to 15%, while the rubbly lavas, peperites, and vesicular basalts exhibited values between 10 and 15% (Marins et al., 2022).

3. Materials and methods

This study included data from a total of 180 wells as well as a 3D seismic survey that covers the Badejo, Pampo, and Linguado oil fields (Fig. 5A). The datasets were provided by the National Agency for Petroleum, Natural Gas, and Biofuels (ANP). Two versions of the 3D seismic volume were analyzed: a time migrated (PSTM; 8 s TWT depth) and a depth migrated (PSDM) volume (Fig. 5A). The seismic data were used to estimate the thickness of the Cabiúnas sequence, the regional faulting constraining the fields, and the position of the overlying Aptian salt layer (Figs. 3, 5, 6, and 7). The methods included the post-processing of the seismic data to enhance its quality and the interpretation of surfaces and regional faults (Figs. 5, 6, and 7), the analysis of well data for the screening of information regarding the Cabiúnas Formation physical parameters (temperature and pore pressure), and the processing of well logs to estimate porosity values.

3.1. Seismic data post-processing

We used the OpenDtex software for the post-processing of the migrated seismic volumes. A dip-steering median filter (SMF) and the fault enhancement filter (FEF) were applied to enhance the quality of the data. We extracted similarity and most positive attributes from the steered data to create new 3D volumes. In addition, a set of conventional filters were applied over the steered data to support the interpretation; this included bandpass frequency filters (3–7 Hz; 7–15 Hz), instantaneous frequency, instantaneous amplitude, and a Hilbert transform. These attribute volumes helped to identify the top of the volcanic sequence and the top of the Precambrian basement, which allowed for an estimation of the regional thickness of the Cabiúnas Formation. The identification of the top of the Cabiúnas Formation was guided by information provided by wells that penetrated this unit (64 wells) (Fig. 5A).

3.2. Analysis of the formation properties

All available legacy data from the wells were analyzed in this study, and we have used the density (RHOB), gamma ray (GR), sonic (DT), and neutron-porosity (NPHI) logs from the wells in the evaluation of the CO₂ sequestration capacity.

Fig. 5A shows the outline of the 3D seismic survey over the Badejo, Linguado, and Pampo fields (Fig. 5) as well as the location of the 64 wells that penetrated the volcanic sequence. We used data from these 64 wells to analyze some of the reservoir characteristics, temperature and pore pressure, that were subsequently used to evaluate the feasibility of CO₂ carbonation in these basaltic rocks (Fig. 5). Specifically, the characteristics of the Cabiúnas Formation were compared to the conditions present in pilot CO₂ mineralization projects to estimate their suitability (Alfredson et al., 2013; McGrail et al., 2014, 2017; Pogge et al., 2019; Clark et al., 2020; White et al., 2020; Ratouis et al., 2022).

3.3. Estimate of volcanic rocks porosity

As the matrix permeability of volcanic rocks is normally very poor, even in rocks with high porosities like vesicular basalts, the permeability of the rocks is primarily controlled by micro- and macro-fracture systems (Lamur et al., 2017; Macente et al., 2019; Tang et al., 2022).

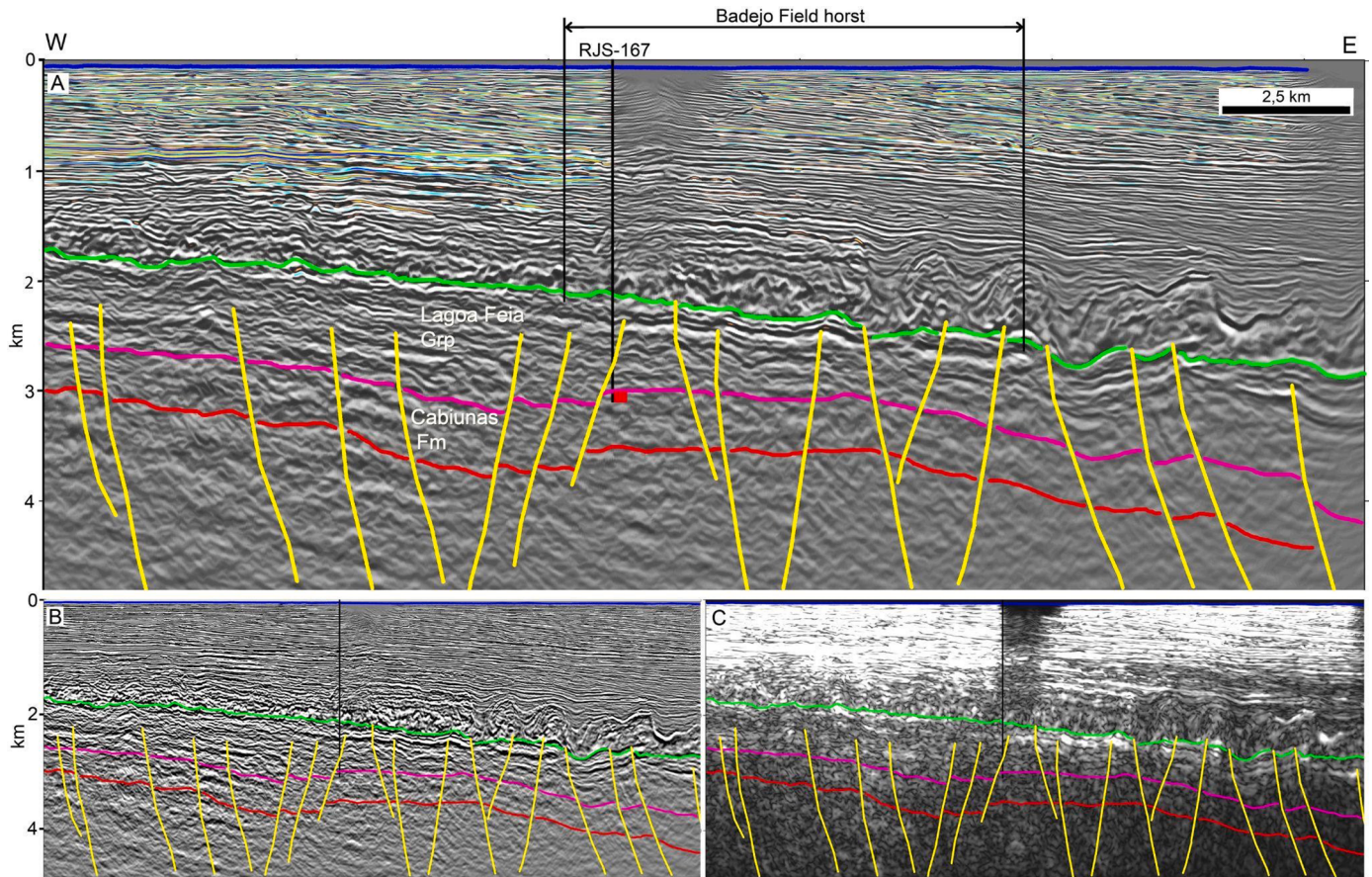


Fig. 6. An arbitrary 2D seismic section extracted from the 3D volume. Interpretation of the top of the Cabíunas Formation is supported by well data, such as the data from RJS-167 as shown in the section, which penetrated approximately 100 m into the volcanic sequence (see the location of the section and the well in Fig. 8A). The section, oriented E-W, also shows the location of the Badejo horst. (A) dip-steered median filter, (B) fault enhancement filter, (C) instantaneous amplitude over steered data. Red horizon – top basement; pink horizon – top of the Cabíunas Formation; green horizon – base of the salt layer; yellow lines – faults.

Calculation of permeability in reservoirs formed by volcanic rocks is very difficult due to the interaction between the original features like vesicles and amygdalites, and later diagenetic features (Zakharova et al., 2012). Both Mizusaki (1986) and Marins et al. (2022) found that the available data was insufficient to assess the permeability associated with the fracture systems of the Cabíunas Formation. Thus, we focused on estimating porosity as it allows for an estimation of the CO₂ storage capacity.

Volcanic reservoirs are generally considered unconventional fractured systems (Gupta et al., 2012; Chaudhary et al., 2022), often possessing complex relationships between original porosity (vesicles, cooling joints) and diagenetic porosity (dissolution and fracturing) (Zahasky et al., 2018; Wang et al., 2018; He et al., 2020). The quantification of porosity in volcanic sequences is often obtained through the modeling of well-log data (Ning et al., 2009; Zakharova et al., 2012; Tang et al., 2022), which allows for an estimation of reserves and flow characteristics. Porosity estimates of basaltic rocks can be obtained through the use of resistivity, acoustic velocity, and density logs (Slagle et al., 2011; Gupta et al., 2012; Asfahani, 2017; Navarro et al., 2020). We used density logs (RHOB) to calculate the apparent porosity of the basaltic rocks of the Cabíunas Formation. This approach allowed us to estimate the bulk porosity of the volcanic intervals, which is related to both primary porosity (vesicles) and diagenetic-related secondary porosity caused by fractures and faults. Gupta et al. (2012) used this technique to estimate the porosity of fractured basalts in onshore and offshore regions of India (Gupta et al., 2012; Chaudhary et al., 2022). McGrail et al. (2011) used a similar approach to define the reservoir intervals in the volcanic sequences of the Columbia River basalts in the

Boise Mill site, which was used for the development of the Wallula CO₂ injection project in Washington, USA (McGrail et al., 2014).

We selected density logs from 14 of the 64 wells investigated in our study (Fig. 5A) to obtain the distribution of the average porosity values across the area sampled by the wells. The calculation also accounts for the general density of basaltic rocks (~2.9 gm/cm³), which was compared to the apparent density taken from the logs using the following equation:

$$\text{Porosity} = \frac{\text{Rhoma} - \text{Rho}}{\text{Rhoma} - \text{Rhof}} \quad (1)$$

where Rhoma is the matrix density, Rho is the bulk density, and Rhof is the fluid density. A fresh basalt with zero porosity was used as the reference matrix. The assumed density of the matrix (Rhoma) was 2.98 gm/cm³, and the fluid density (Rhof) was assumed to be 1 gm/cm³ (Gupta et al., 2012; Chaudhary et al., 2022).

The sequestration capacity, in terms of the potential volume of CO₂ able to be sequestered, was accomplished following recent methods used in other volcanic sequences that also represent fractured reservoirs (Koukouzas et al., 2019; Raza et al., 2022). The sequestration capacity of sedimentary rocks via injection methods is dependent on many parameters (depth, pore pressure, temperature, mineralogy, and formation fluids) (Ajayi et al., 2019). For depleted oil and gas reservoirs, a simple method to estimate the storage capacity is based on the calculation of the volume of fluids produced as well as the water and gas injected during the recovery stages (Rockett et al., 2013; Raza et al., 2022). The volume of fluids produced can be used to estimate the injection capacity of compressed CO₂. The limit of injectable supercritical CO₂, in

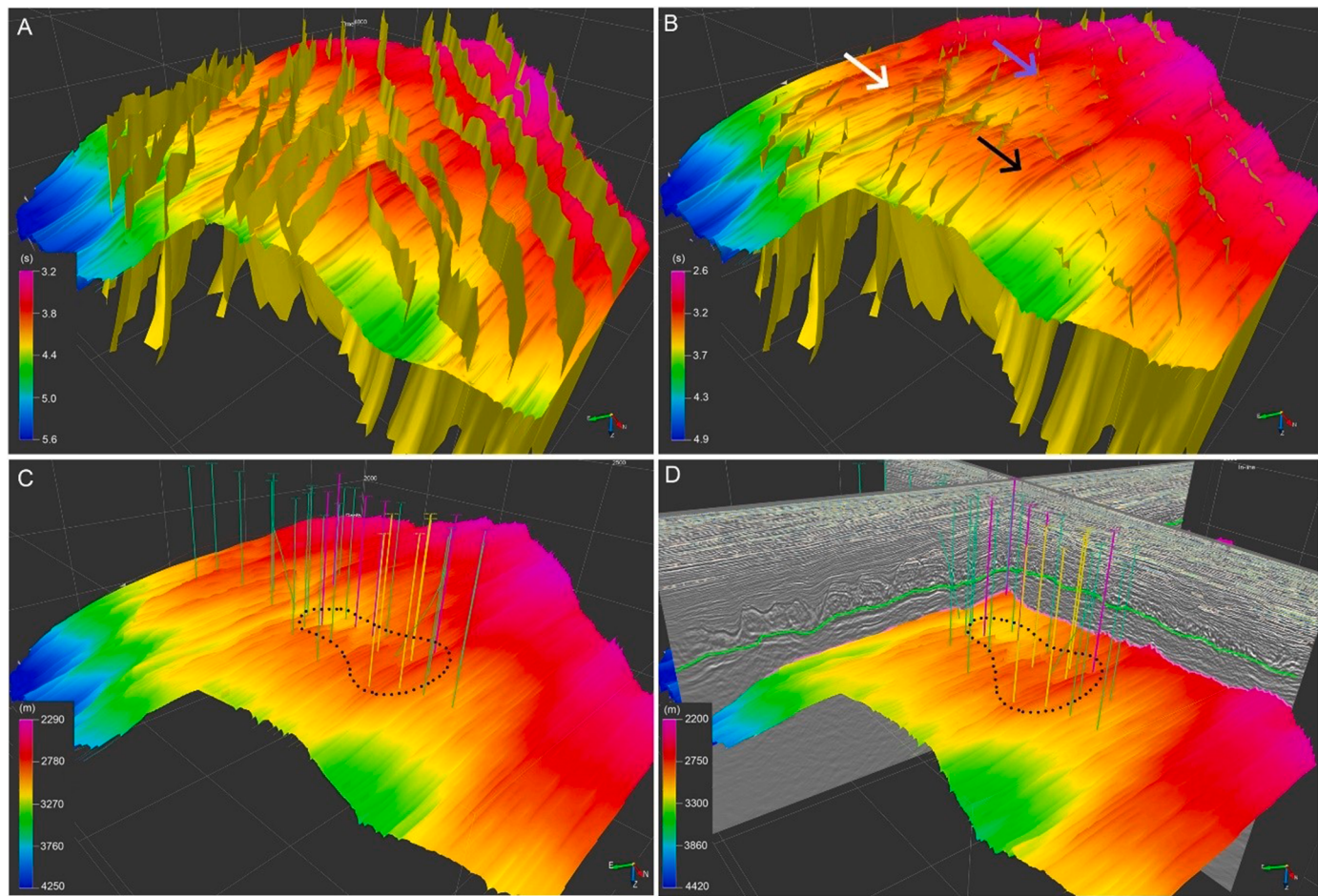


Fig. 7. Interpretations of the surfaces of the (A) top of the basement (depth in time) and the (B) top of the Cabiúnas Formation (depth in time) were mapped onto the 3D seismic survey. The yellow 2D planes represent the main rift fault zones. The black, blue, and white arrows show the location of the Badejo, Linguado, and Pampo horsts, respectively. (C) The surface of the top of the Cabiúnas Formation and the wells used for the estimation of the CO₂ storage capacity (depth in meters). The polygon delineated by the black dotted line indicates the target zone chosen for the estimation of the storage capacity (yellow vertical lines – oil well producers from basalt; purple vertical lines – the non-commercial discovery of oil in basalts; green vertical lines – other wells used to estimate storage capacity in this study). (D) Surface of the top of the Cabiúnas Formation as well as 2D seismic sections showing the position of the base of the regional salt layer atop the Lagoa Feia Group (green horizon).

conventional reservoirs composed of sedimentary rocks is also constrained by the hydrostatic pressure because the seal capacity may be compromised due to overpressure (Alcalde et al., 2018; Zappone et al., 2021).

However, it is difficult to make assumptions about the produced volume in volcanic reservoirs composed of crystalline rocks (Raza et al., 2022). Thus, we adopted a simplified volumetric method to estimate the storage capacity of the rocks, which utilizes the porosity parameter obtained through density logs, as described above. The volumetric approach was adopted by McGrail et al. (2006) to calculate the CO₂ storage capacity for the Columbia River basalt, and it provided a tentative approach for this estimate. This method is based on the experience provided by the US Department of Energy, which studied the remediation of aquifers in basaltic rocks, and it involves the average thickness, average porosity, and average formation pressure of the rock mass treated for injection to obtain a reliable estimate for CO₂ storage (Raza et al., 2022). This technique was also used by Anthonsen et al. (2014) to estimate storage capacity in volcanic rocks in Iceland. We adopted the volumetric method approach described by Koukousas et al. (2019), who studied the CO₂ storage potential of basaltic rocks in Greece, to estimate the volume capacity of an area of the Badejo Field:

$$\text{CapacityStorage} = \sum(V \times \varphi \times \rho \times \varepsilon) \quad (2)$$

where V is the volume of the basaltic rocks, φ is the average porosity, ρ is the specific gravity of the saturated CO₂, and ε is the CO₂ storage ratio for the basaltic rocks. The storage ratio refers to the percentage of CO₂ in the mass injected into the reservoir (%-CO₂ dissolved in the water) based on the results of the CarbFix pilot project in Iceland (Gislason et al., 2014). This ratio was defined based on the limitations associated with the volume of water available for injection in this onshore project (Gislason et al., 2014). Koukousas et al. (2019) also adopted a value of 5% for the estimation of CO₂ sequestration in basaltic rocks in Greece. However, we adopted two ratios for our estimate: 5% and 10% of the injected mass because in offshore projects the availability of water for the CO₂ dissolution is not limited. The specific gravity of CO₂ (716.55 kg/m³) was defined based on the work of Span and Wagner (1996), based on average values of parameters of the Cabiúnas such as depth of the hypothetical reservoir interval, 30 MPa for the formation pressure, and 90 °C for the reservoir temperature.

Our calculation of storage capacity did not consider the time for the injection process. Some works have addressed the possible effect of porosity reduction due to the cumulative injection of CO₂ on the reservoir and the secondary mineralization. A decrease in the porosity during the development will impact the previous calculation of the porosity that can be used to store the gas. Many aspects need to be considered to predict the effect of mineral dissolution and secondary mineral phases

formation (Gunnarson et al., 218) – the complex reactive transport framework (Tutolo et al., 2021) and even aspects like the natural fracture topology could impact the flow of the CO₂ and the mineralization (Wu et al., 2021). Laboratory experiments demonstrated that process like micro fracture-induced mineralization plays an important role in the self-sustainability of the reactions (Xing et al., 2018), and flow-through experiments in basalt samples demonstrated that the porosity decreases slightly (~0.7 to 0.8%) and it could even increase in some cases (Luhmann et al., 2017). As stated by Gunnarson et al. (2018), we just don't have sufficient data at present to completely understand the long-term effects of these complex interactions on the reservoir regarding large injection projects. In this context, we have considered a conservative approach for the calculation of the volume that could be injected in the studied rocks.

4. Results

Of the 64 wells studied, seven wells recorded the occurrence of non-commercial oil, and five wells were oil producers (Guardado et al., 2000). Fig. 5A shows the four zones (A–D) proposed by Mizusaki et al. (1988). They are oriented NNE–SSE and represent the dominant subaerial to subaqueous conditions that were present during the formation of the Cabiúnas deposits. The oil producers were found in the sectors associated with subaerial deposition. The interpolation of the Cabiúnas depth record in the 64 wells studied allowed us to obtain a regional configuration of the depth to the top of the volcanic sequence (Fig. 5B). The contour map of the top of the Cabiúnas also showed that the oil fields (Badejo, Linguado, and Pampo) formed above three horsts on the southeastern border of the Badejo High (Fig. 3). The depth to the top of the Cabiúnas Formation in the production wells in the Badejo Field ranges from 2800–3,100 m, and the three horsts are bounded by primary faults trending NE–SW and secondary faults trending ENE–WSW (Fig. 5B). Temperatures recorded within the Cabiúnas Formation range between ~80–110 °C. Temperatures were found to be higher in the Badejo Field region, and the temperature patterns show two zones with higher values trending N–S and E–W (Fig. 5C). The regional faults interpreted in the 3D seismic data are shown in the maps of Fig. 5, and the relationship between the variations in the studied parameter values and the orientation of the faults suggests the structural compartmentalization of these properties. This is mainly observed for the temperature values in the Badejo Field. Data collected on formation pressure showed that the Badejo horst also exhibited higher values, ranging from ~15–37 MPa. The formation pressure exhibited compartmentalized patterns similar to those observed in the temperature profiles, reinforcing the possibility of a tectonic control on the compartmentalization observed in the temperature values (Fig. 5D).

4.1. Storage capacity modeling using seismic and well data

Fig. 6 shows an interpretation of an arbitrary 2D seismic section extracted from the 3D volume, supported by the information recorded in well RJS-167. The interpretation of the top of the Precambrian basement is shown based on three different representations of the original seismic data, obtained through the use of filters and attributes (Fig. 6). The Badejo horst, located on the eastern border of the Badejo High (Fig. 3), is also highlighted.

Fig. 7 shows the interpreted surface of the top of the basement and the surface of the top of the Cabiúnas Formation. The seismic data interpretation constrained the morphological configuration of the three horsts associated with the Badejo, Linguado, and Pampo oil fields (Fig. 7). The black, blue, and white arrows in Fig. 7B indicate the locations of the Badejo, Linguado, and Pampo horsts, respectively. The main faults formed by the rift event that cut the Cabiúnas Formation were mapped. These faults were paths by which the oil and gas migrated from the lacustrine source rocks of the rift sequence to the upper sequences (Guardado et al., 1990; 2000). The yellow planes in Fig. 7A and

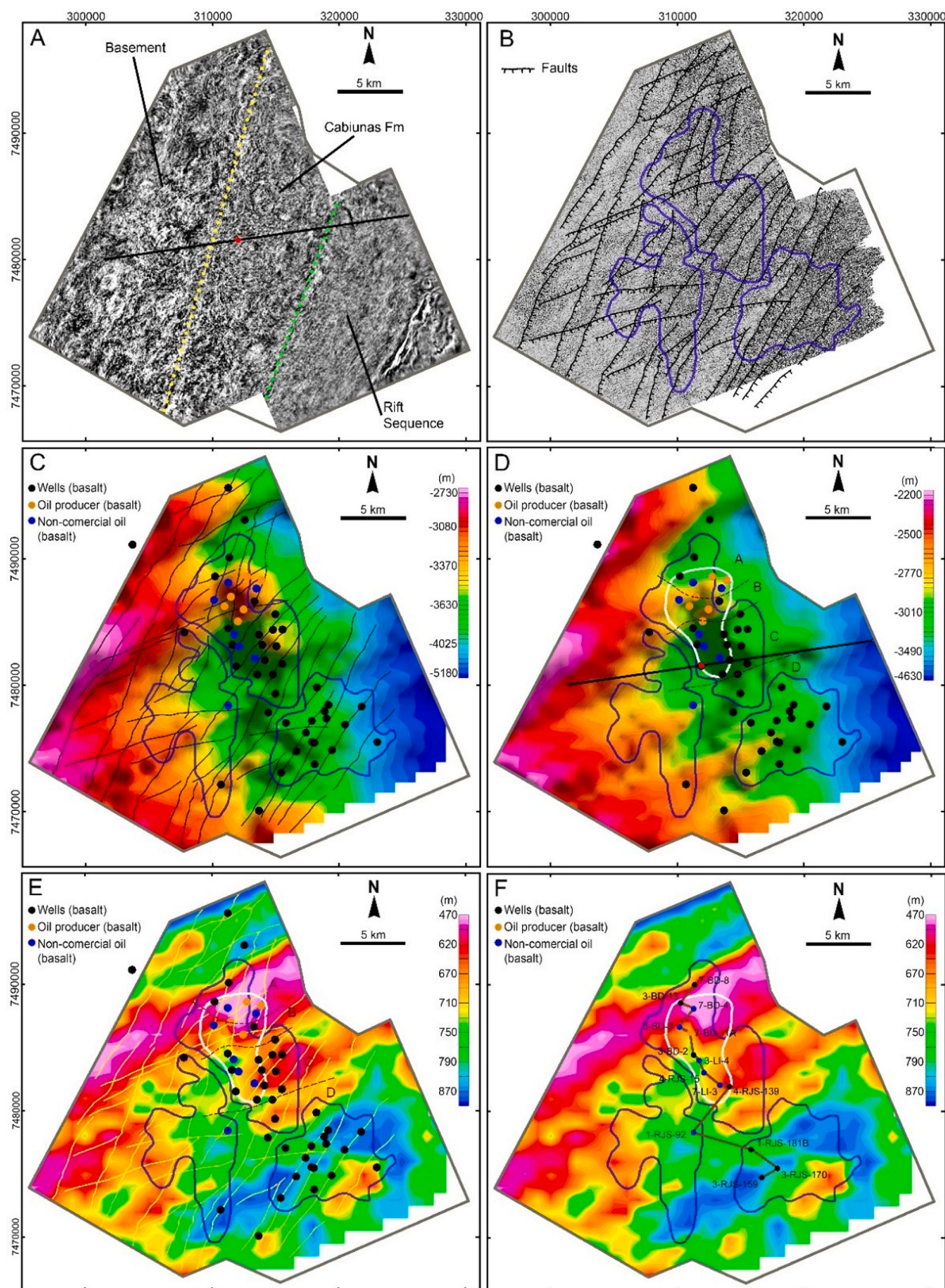
7B indicates the rift faults that cut the Cabiúnas sequence. The lateral contact of the Cabiúnas rocks with the overlying source rocks due to the rifting process was the primary mechanism by which the oil migrated to the volcanic sequence of the Badejo horst (Guardado et al., 1990; 2000) (Figs. 3 and 6). The fluid charging of the Badejo horst also suggests that these rocks possessed some level of permeability that allowed the oil to accumulate. Taking this into account, we defined an arbitrary area around the oil-producing wells in the Badejo horst within which we built a hypothetical model for the estimation of the CO₂ injection storage capacity (polygon indicated using dotted black line) (Fig. 7C and 7D). Fig. 7D shows that the Cabiúnas deposits in the selected area in the Badejo horst is capped by the Lagoa Feia Group deposits (Fig. 3), including interbedded shales and the upper salt layer (green horizon), all of which represent regional seals (Fig. 6). The Fig. 7 shows that selection of target zones for CO₂ injection will need to model tectono-stratigraphic aspects like the location of horsts and the fault compartmentalization.

Fig. 8 shows the regional characteristics of the Cabiúnas Formation in the study region. Fig. 8A shows a time slice positioned at 4000 ms in the 3D seismic survey. Due to the gentle dipping of the basement that underlies the Cabiúnas Formation and Lagoa Feia Group succession, the seismic facies of these three lithosequences are shown by the horizontal cut of the time slice from west to east. It shows that the regional distribution of the Cabiúnas rocks covers the platform of the Campos Basin. Fig. 8B shows the interpreted surface of the top of the Cabiúnas Formation with the most positive curvature attribute, which helped to map the fault zones which controlled the compartmentalization of the reservoirs found in this region (black lines). Rift faults extend from the basement through the Cabiúnas succession to the base of the Lagoa Feia Group (Fig. 6). The darker areas indicate zones with more occurrence of natural fractures, which are critical for flow modeling of possible CCS projects. Fig. 8C and 8D show 2D shaded relief contour maps of the top of the basement and the Cabiúnas Formation. The three horsts related to the three oil fields are positioned on the border of Badejo High. The Badejo horst exhibits a more prominent basement topography, which could have been a key reason for the accumulation of oil in the volcanic rocks in this region. Fig. 8E and 8F show the tentative estimation of the thickness of the Cabiúnas Formation in the study area, which varies between 450 and 1000 m. The formation thickness will be a controlling factor for CCS projects' site selection and the volumes which could be injected into the basaltic rocks. In the arbitrary area defined over the Badejo horst, the Cabiúnas Thickness varies between ~500–700 m (Fig. 8E and 8F). The production wells are located in the sector that was subject to subaerial conditions during deposition (Zones A–B) (Mizusaki et al., 1988), while the wells drilled through the Linguado and Pampo sectors either found non-commercial oil or were dry. The Badejo horst appears to be the sector that is most compartmentalized by faults (Fig. 8B). The arbitrary zone used for the calculation of the storage capacity is shown in Fig. 8E and 8F (polygon delineated by white lines) and includes both the production wells and the non-commercial findings (Fig. 8E and 8F). Fig. 8F shows the section (brown line) formed by the 14 wells chosen for the estimation of porosity distribution within the volcanic sequence, which allowed for a reliable calculation of the storage capacity. This is the same sequence of wells that Mizusaki et al. (1988) used to describe the geological characteristics of the rocks sampled in the Cabiúnas Formation. The section trends with NNW–SSE and includes wells from the Badejo, Linguado, and Pampo fields.

The results showed above demonstrated that the site selection for CO₂ storage should consider regional structural control and paleogeography, which controlled environmental conditions during the formation of the Cabiúnas deposits.

4.2. Estimation of storage capacity

Fig. 9 shows the section constructed from the profiles of 14 wells, including boreholes from the Badejo, Linguado, and Pampo fields.



(caption on next page)

Fig. 8. (A) Time slice at 4000 ms of the 3D seismic survey (FEF volume). The yellow and green dotted lines mark the separation between the basement rocks, the Cabiúnas Formation, and the Lagoa Feia Group, characterized by different patterns of seismic facies. The black line and the red dot indicate the position of the arbitrary 2D seismic section and the location of the RJS-167 well shown in Fig. 6. (B) The interpreted surface of the top of Cabiúnas Formation shows the most positive curvature attribute, which helped to map the faults and indicates the intensely fractured zones (darker areas). The black lines show the projection of the rift fault planes trending primarily NE–SW and secondarily ENE–WSW. (C) Basement depth contour map (meters) of the rift faults. (D) Contour map of the depth to the Cabiúnas Formation (meters). The white polygon indicates the area selected around some wells across the Badejo horst used to constrain the hypothetical model used to estimate the CO₂ storage capacity. (E and F) Estimated Cabiúnas Formation isopach maps. The brown line indicates the location of the section that connects the 14 wells used to calculate the porosity logs presented in Fig. 9.

RHOB logs were used to create a new porosity log for the rocks of the Cabiúnas Formation. The wells correlation section trends roughly from NNW–SSE (Fig. 9). The profile of the wells also contained the gamma-ray and the NPHI logs, which are presented together with the porosity log. The section allows us to observe the variation in the depth to the top of the volcanic sequence across the three fields, which is associated with the basement horsts bounded by the faults that cut the overlying Cabiúnas Formation (Figs. 3 and 6).

We also integrated the lithofacies description provided by Mizusaki et al. (1988) into four wells in this section. Their descriptions were based on an analysis of the cores sampled (Fig. 10), allowing us to investigate the correlation between the apparent porosity results and the distribution of lithofacies as previously interpreted by these authors, which can aid future work on reservoir characterization.

There were several interesting positive and negative correlations between the porosity logs and the other logs (GR, NPHI and DT) showed in Fig. 9, possibly caused not only by the lithological variation and diagenesis but also by deposition conditions and early alteration (Mizusaki et al., 1988; Marins et al., 2022). Intervals with porosities ranging between 10 and 20% are widely distributed (Fig. 9). In some wells, these intervals are tens of meters thick; this is important with regard to the reservoir interval volume, especially in the Badejo wells. Wells RJS-181B and RJS-170 in the Pampo Field showed the worst cases of porosity distribution, with many intervals ranging between 0 and 10%. In the Badejo field, some wells (7-BD4 and 3BD-3) possessed thin intervals of volcanic rocks with apparent porosities between 30 and 40% (Fig. 9).

In general, low gamma ray values were correlated with higher density values and, consequently, with lower porosity. However, there were local examples of low gamma ray values that were associated with low-density values and high apparent porosity ranges (RJS-92; Fig. 9). The NPHI log shows that there is a minor positive correlation between high neutronic counts and low-density intervals that potentially contain more fluids (fractures, vesicles, and vugs), especially in the wells drilled in the Badejo field. However, in the wells at the southeastern end of the section (Pampo Field), higher NPHI values are also locally related to intervals with low porosity (RJS-170 and RJS-159 wells). The sonic (DT) log shows that there is a positive correlation between lower Δt values, higher Rhob values, and lower apparent porosity ranges (0–10%). Higher sonic log values are generally associated with low-density rocks and normally indicate higher porosity intervals (Fig. 9). Some of the punctual contradictory patterns can be associated with problems related to the original borehole data acquisition.

The porosity logs reveal the high vertical compartmentalization of the porous intervals. High porous intervals are more frequent in the Badejo Field, compared to the porosity distribution of the Linguado and the Pampo fields. Some sectors show an incipient cyclicity that may be associated with successive lava flows produced by the effusive processes that built the succession. The intercalation of thick intervals with greater porosities with intervals with low porosity values in the wells of the Badejo and Linguado fields highlight the complexity of the relationship between the porosity and lithofacies distributions (Fig. 9). There is no discernible pattern in the vertical variation between the wells regarding the continuity of possible reservoir intervals or flow units.

Fig. 10 shows four well profiles from the geological section shown in Fig. 9, including the GR, RHOB, and porosity logs, as well as a color bar representing an interpretation of lithofacies provided by Mizusaki et al.

(1988). This lithofacies description covers each of the cored intervals, and these four wells were chosen because they represent the larger cored intervals across the sampled boreholes. The most representative lithologies are basalt flows that can be classified into two categories: 1) gray lavas, which were less affected by subaerial exposure and 2) red lavas, which show evidence of weathering, such as oxidation and meteoric diagenesis, before burial (Mizusaki, 1986; Mizusaki et al., 1988). The correlation between the porosity estimates and the lithologies showed that sedimentary rocks, volcaniclastic rocks, and breccias generally represent low porosity intervals, with few exceptions such as in well BD-11A.

As reported by Mizusaki et al. (1988), red lava flows were generally correlated to high porosity intervals, especially in the Badejo Field wells. However, they were less represented in the sampled intervals in terms of thickness. Gray lava flows were correlated with low to medium porosity intervals; a good example of this was a thick vertical interval in the BD-11A well, which exhibited low porosity values (Fig. 10). Apparent porosity values are influenced by both primary features, such as vesicles, and late diagenetic structures, such as faults, fractures, and dissolution cavities. Since there was no specific relationship between the porosity and the lithologies described in the sampled intervals, this suggests the strong influence of diagenetic factors.

The six wells with the greatest penetration depths into the Cabiúnas Formation were used to define the vertical range of porosity values (Table 1). This allows for the estimation of the vertical section of a hypothetical interval for a given average porosity. The hypothetical scenario was comprised of a 3D volume formed by the perimeter shown in Fig. 8D, representing an area of 31 km² that covers the Badejo Field and a total reservoir thickness of 300 m for fluid injection. We calculated the probable interval thickness with isotropic porosities of 10%, 15%, and 20% using the mean values extracted from the porosity logs from the six wells (Table 1). The scenarios assumed were very conservative based on the ranges adopted, considering that porosity values in basaltic formations normally ranges from 10% to >60% (Andrews, 2022; Chaudhary et al., 2022). For example, the total sampled thickness used to estimate mean values is approximately 678 m. Using a threshold value of 10%, we found that 440 m of the vertical rock sequence exceeded this value, representing ~73% of the total thickness; i.e., the interval containing porosity values equal to or higher than 10% based on the porosity logs. Thus, we adopted a thickness of 231 m for the first scenario (10% porosity) because it represents approximately 73% of the 300 m thickness of the general hypothetical reservoir (Table 2). In reality, the interval would exhibit a higher total porosity than we assumed in the isotropic scenario with an isotropic value. Table 2 shows the injection scenarios based on the estimated thickness calculated from the threshold porosity values of 10%, 15%, and 20%. Based on the assumed compressibility limits and the %CO₂ in the injected water (5% and 10%), we calculated storage capacity values ranging from 15.8 to 23.4 Mt and 31.7–47 Mt for 5% and 10% diluted CO₂, respectively (Table 2). These results indicates that the sequestration capacity could be even higher if the real range of porosity values is considered. This is especially important because higher porosity will potentially imply better injectivity conditions. In addition, as observed in the Wallula project, the selection of intervals with greater porosity values (15–25%) (injection zones) should be done while taking into account the occurrence of intervals with much lower porosity that can act as cap rocks (McGrail et al., 2011; White et al., 2020).

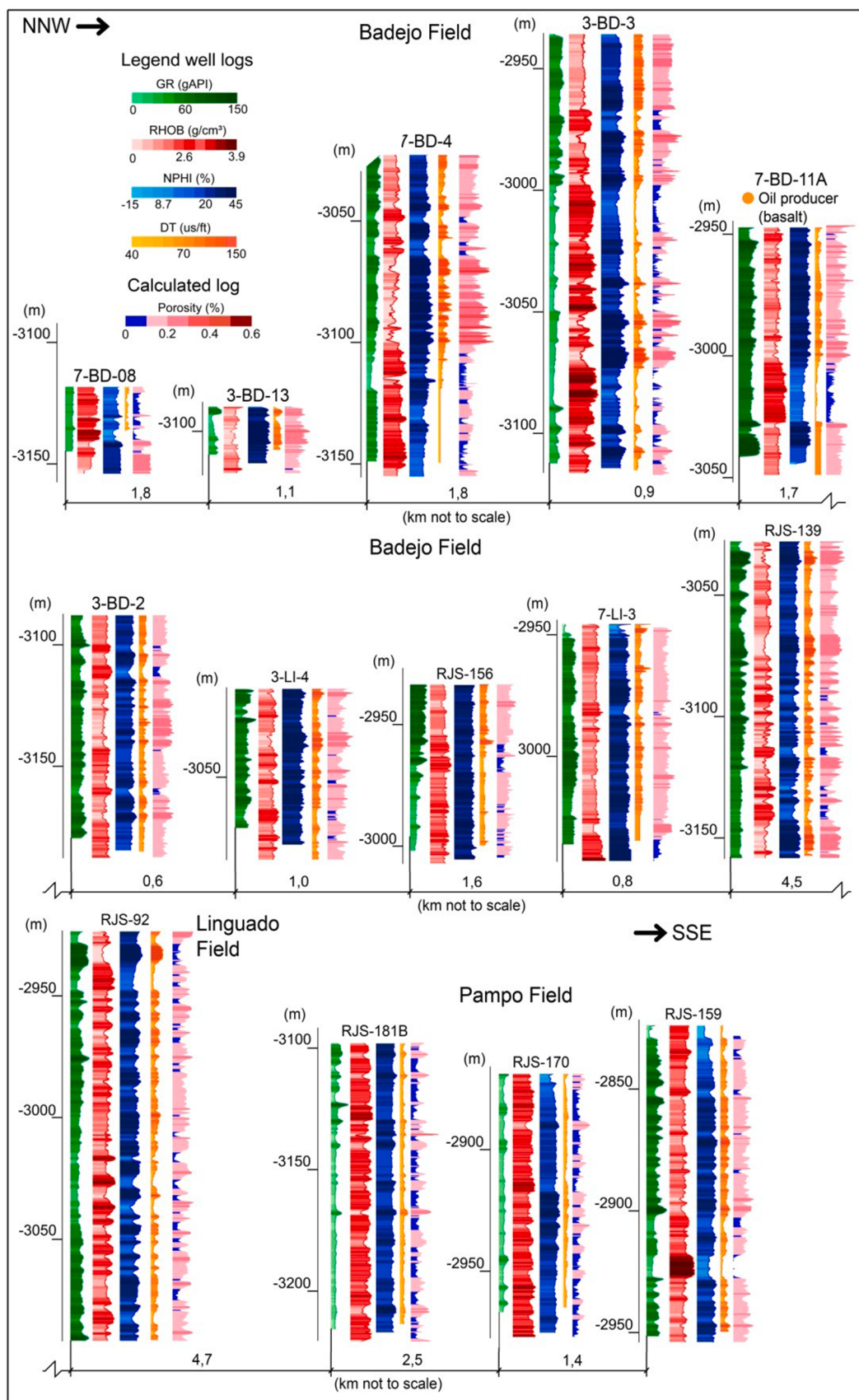


Fig. 9. Geologic section of 14 wells across the Badejo, Linguado, and Pampo fields (see Fig. 8F for the location of these wells). (A) Well profiles show the GR, RHOB, NPHI, DT, and porosity logs. The depth to the top of the Cabiúnas Formation was obtained from borehole records. Well 7-BD-11A was an oil producer from basalts in the Badejo field.

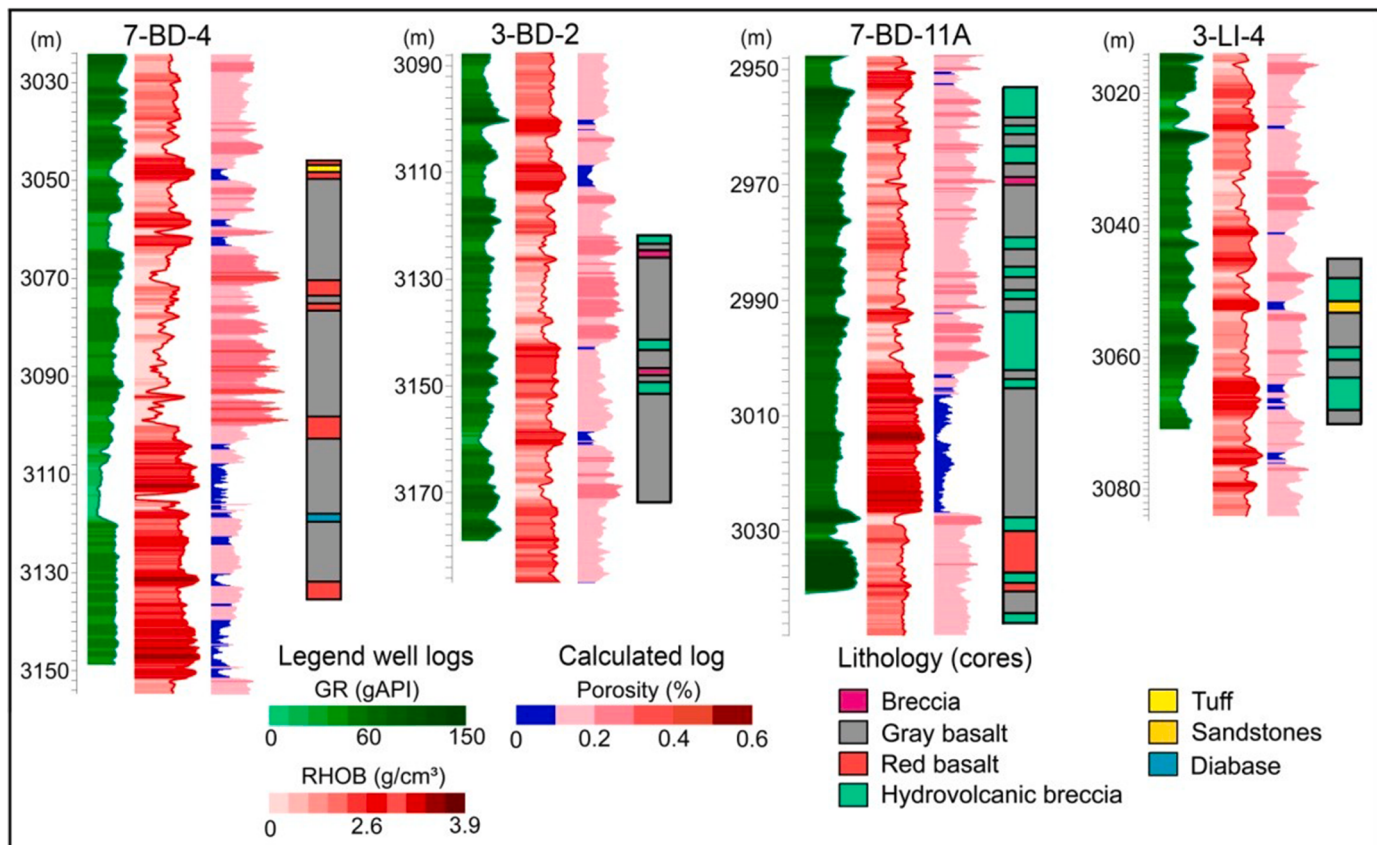


Fig. 10. Details of four wells shown in Fig. 9 and how they relate to the lithofacies distribution proposed by Mizusaki et al. (1988) from core analysis. The gray basalt and reddish basalts (with subaerial alteration) exhibit good porosity values.

5. Discussion

Data provided by the wells which penetrated the Cabiúnas Formation showed that the temperature and pressure zones within the basaltic sequence are compartmentalized by faults (Fig. 5). The temperature of the Cabiúnas rocks at the Badejo Field (Fig. 5) ranged from 75 to 108 °C. According to Gadikota et al. (2021), experimental evidence suggests the complete conversion of calcium silicate (CaSiO_3) and the >80% conversion of magnesium silicate (Mg_2SiO_4) to their respective carbonates occur at temperatures between 150 and 200 °C. Tutolo et al. (2021) argued that many of the experiments developed so far provided valuable data on the conditions and reaction effects of silicate minerals in basaltic rocks. However, the controlled alkalinity budget through the high content of NaHCO_3 or KHCO_3 used in the experiments is orders of magnitude different from the real-world subsurface operations. The authors also argued that some experiments using deionized water also showed that the mineralization is feasible, but the differences between controlled experiments and the field-scale projects using diluted or supercritical CO_2 need to be reconsidered.

Also based on experiments and field studies, Gadikota et al. (2021) suggested that the optimal conditions for mineralization in basaltic formations occur at high temperatures between 100 and 220 °C and at partial CO_2 pressures between 5 and 20 MPa. The olivine is highly reactive and its optimal temperature for carbon mineralization is ~180 °C (Raza et al., 2022). Marieni et al. (2021) showed that the most efficient temperature range for carbonation in seawater systems was 25–170 °C and that the optimal limit was below 260 °C. In addition, pilot projects in Iceland and Washington, USA have shown that the ideal temperature range for carbonation lies between 25 and 250 °C and that temperatures higher than 100 °C accelerate the process (Clark et al., 2020; Marieni et al., 2021; Raza et al., 2022). Higher temperatures also

limit any biological activity that might harm the injectivity and the carbonation reactions (Gunnarson et al., 2018). According to these latter authors, CO_2 is 15% less soluble in seawater than in freshwater, but seawater accelerates the dissolution process in these rocks. Thus, the use of seawater for injection is feasible. The availability of seawater in the context of offshore projects also reduces storage costs.

The formation pressure of the volcanic rocks in the Badejo Field also appears to be compartmentalized, with significant changes of pressure values marked by faults, suggesting that fault zones controlled the fluid migration and the trapping of fluids in the syn-rift reservoir, consistent with the model described by Guardado et al. (1990). Analysis of well data showed that formation fluid pressure ranged from 25 to 38 MPa, with an average value of 30–32 MPa. Successful mineral carbonation projects (onshore) were conducted in geological formations with hydrostatic pressures ranging from 2.5 to ~16 MPa (Table 3). Mineralization processes in mafic rocks are still not completely understood (Raza et al., 2022). However, experimental studies with controlled temperatures, CO_2 saturations, and fluid pressures have shown that high pressures increase the solubility of CO_2 in water as well as the dissolution rate of volcanic glass and minerals (Kelemen et al., 2019; Raza et al., 2022). Experiments have shown that temperatures greater than 50 °C and CO_2 partial pressure greater than ~20 MPa resulted in the more rapid dissolution of minerals and higher rates of mineralization (Gíslason et al., 2018; Clark et al., 2020; Raza et al., 2022). Indeed, greater reservoir depths, temperatures, and hydrostatic pressures mean that less water is required to achieve CO_2 dissolution and the expected reactive effects for the carbonation process. According to Gunnarson et al. (2018), at a pressure of 25 bars and a temperature of 25 °C, approximately 27 tons of pure water is required to dissolve a ton of CO_2 gas either before or during the injection. This showcases the advantage of higher hydrostatic pressures during injections with respect to the

Table 1

Porosity estimates from the 14 wells selected for storage capacity estimation. Porosity estimates of the wells marked in red were used to define the thickness of the intervals possessing the threshold porosity values outlined by the three hypothetical scenarios.

Well ID	Cabiúnas Drilled thickness (m)	Interval thickness with $\geq 10\%$ Porosity	Interval thickness with $\geq 15\%$ Porosity	Interval thickness with $\geq 20\%$ Porosity
7 BD 8 RJS	37	20.5 (40%)	13.2 (14.3%)	11.5 (8.2%)
3 BD 13 RJS	48	42.5 (85%)	37 (71.7%)	23.7 (37.6%)
7 BD 4 RJS	133	109.8 (79.7%)	83.6 (60.6%)	48.2 (35%)
3 BD 3 RJS	196	123.1 (59.6%)	93.5 (43.3%)	54.9 (22%)
7 BD 11A RJS	101	79.1 (78.2%)	61 (60.3%)	18.2 (17.8%)
3 BD 2 RJS	104	97.2 (93.2%)	71.5 (67.5%)	31.4 (27.3%)
3 LI 4 RJS	76	70.6 (92.7%)	54.6 (71%)	21.4 (26%)
4 RJS 156 RJS	69	57.2 (81.7%)	39.8 (54.6%)	12.6 (12.4%)
7 LI 3 RJS	97	87.8 (90.5%)	68.7 (70.8%)	16.1 (16.5%)
4 RJS 139 RJS	137	124 (90.5%)	62.6 (45.5%)	60.2 (43.8%)
1 RJS 92 RJS	195	155 (78.6%)	114.8 (57%)	55.7 (25.3%)
1 RJS 181B RJS	126	63.6 (49.6%)	30.3 (33.6%)	13.5 (9%)
3 RJS 170 RJS	108	46.2 (42.8%)	12.6 (11.6%)	2.5 (2.2%)
3 RJS 159 RJS	126	103 (81.7%)	67 (53.1%)	13.6 (10.6%)
Total	1553	1179.6 (76%)	810.2 (52%)	383.5 (24.6%)

Table 2

Storage capacity estimations of the hypothetical zone. The hypothetical interval has a thickness of 300 m and an area of 31 km². The probable thickness of the intervals that exhibit a porosity of 10%, 15%, and 20% were calculated based on the proportion of the selected wells that exhibited values equal to or greater than the stated thresholds. In each scenario, the estimated storage capacity is presented Mt.

	Probable thickness with porosity $\geq 10\%$	Probable thickness with porosity $\geq 15\%$	Probable thickness with porosity $\geq 20\%$
Drilling interval 300 m	213	138	72
Storage Capacity Mton (5% diluted CO ₂)	23,4	22,8	15,8
Storage Capacity Mton (10% diluted CO ₂)	47	45,6	31,7

solubility of CO₂.

A main concern regarding the injection process is the possibility of pressure buildup due to the permeability of the reservoir, and the infiltration rate will control the rock dissolution and define the viability of the mineralization (Gíslason et al., 2014; Clark et al., 2020; Raza et al., 2022). However, the available data in the Cabiúnas Formation is insufficient to conduct any detailed investigations; these factors should be investigated in future experimental or numerical studies and new

Table 3

Physical characteristics of the geological systems of basaltic rocks used for CO₂ mineral carbonation of pilot projects compared with properties of the Cabiúnas Formation (Gíslason et al., 2010; Zakharova et al., 2012; Lavalleur and Colwell, 2013; McGrail et al., 2017; Clark et al., 2018; Gunnarsson et al., 2018; Schwartz, 2018; Marieni et al., 2021).

Projects	Avg. Temp (°C)	Avg pH	Avg Pressure (MPa)	Depth (m)	Porosity (%)
CarbFix 1	35 (20–50)	10 (9–11)	2.5 (350 m)	530	5 - 40
CarbFix 2	~250 (220 - 260)	7.17	16.7 (2000 m)	1900 - 2200	8 - 10
Wallula	45.5 (37–54)	9.55 (9–10.1)	7.5 (7–8)	830 - 890	15 - 45
Cabiúnas	90	7.14	32.46	2930 - 3260	10 - 40

drilling operations.

The pH of the solution in the reservoir is a key factor that affects the dissolution rate of the rocks (glass and minerals) (Kelemen et al., 2020; Raza et al., 2022). Besides the partial pressure of CO₂ and the temperature, alkalinity and salinity of the water are also primary drivers (Gíslason et al., 2010). According to these authors, ultramafic and basaltic rocks such as gabbros and basaltic glass, which are rich in divalent cations and poor in silica, have relatively quick dissolution rates, with cation release rates that are approximately two orders of magnitude greater than that of granite and rhyolite. Dissolution of glassy rocks release Ca²⁺ results in an increase in pH of formation fluids from as low as 4–6 to values as high as 7–9. Thus, water in contact with basaltic glasses and ultramafic rocks, sealed off from atmospheric CO₂ or other CO₂ sources, exhibits high pH values ranging from 9 to 11 (Gíslason et al., 2010) (Table 3). Available data about the Cabiúnas Formation suggest that the water has pH values of ~7, which is favorable for CO₂ mineralization as discussed above (Table 3) (Supplementary material). Table 3 shows a comparison between the chemical and physical parameters of basaltic formations where CO₂ carbonation projects were developed and the parameters of the Cabiúnas Formation.

The interpretation of seismic data allowed for the estimation of the thickness of the Cabiúnas Formation (Figs. 6, 7, and 8), which varies between 1000 m in some grabens to 400–500 m over the basement horsts that form the Badejo Field (Fig. 8). This allowed us to understand the effects of the compartmentalization produced by the rift faults that cut through the volcanic succession and showed that the thickness of the Cabiúnas deposits is capable of hosting injection projects with multiple injection intervals. This interpretation, in conjunction with well data, also showed that the regions above horsts bounded by faults (Figs. 6 and 8) represent the best option for injection projects. Evidence of previous fluid migration into these zones indicates that they have more ideal reservoir qualities (porosity and permeability). This is also consistent with the oil-producing wells in the basalts above the horst that form the Badejo Field (Figs. 6 and 8). Based on these conditions, we estimated the storage capacity of this region for carbon sequestration (white polygon; Fig. 8D and 8E). The apparent porosity extracted from the RHOB log was useful in understanding the general relationship between porosity and lithofacies distribution (Fig. 9) and the analysis of the porosity of the 14 wells across the three fields allowed us to gain a rough understanding of the porosity distribution in the Cabiúnas deposits (Fig. 9). The estimated porosity accounts for features such as primary vesicles, explosive fractures, shrinkage fractures, as well as secondary pores and fractures (Tang et al., 2022). Recent work on the characteristics of basaltic oil reservoirs has suggested that fractures and late dissolution play an important role in fluid flow (Tang et al., 2022). Since the permeability of rock matrix of basaltic rocks are low, secondary fracturing and diagenetic aspects play an important role in reservoir permeability (Barreto et al., 2017; Tang et al., 2022). In terms of porosity, the location of the best reservoir zones is influenced by primary fractures related to the

architecture of the successions, which includes lava flows and other lithologies. The processes of cooling, gas release, and primary fracturing forms zones of high porosity at specific intervals within the lava flow (Mizusaki et al., 1988; Guardado et al., 1990; Reis et al., 2013; Barreto et al., 2017; Tang et al., 2022). Explosive fracturing and auto-brecciation also are important factors; however, the authigenic formation of minerals and compaction tends to reduce the porosity in these types of lithologies, especially in burial depths above 3 km (Tang et al., 2022).

The analysis of the porosity logs showed that the basaltic sequence in the Badejo and Linguado fields were the most ideal, with thick vertical zones with higher porosity (Fig. 9). Mizusaki et al. (1988) suggested that the reservoir conditions were controlled by aspects associated with their deposition across four distinct environments. This is consistent with our analysis of the porosity logs. However, the influence of diagenetic processes should be considered in future studies (Marins et al., 2022). Mizusaki et al. (1988) suggested that reddened lavas possessed higher porosities because they were formed in subaerial conditions, where early alteration before burial resulted in their erosion, dissolution, and oxidation (reddish deposits). In contrast, the gray lavas were formed in subaqueous conditions and were not exposed to weathering, resulting in lower porosities (Mizusaki et al., 1988). We compared the interpretation of the core samples by Mizusaki et al. (1988) (Fig. 10) with the porosity logs and agree with their interpretation of the relationship between the reddened lavas and high porosity. However, we found that gray lavas exhibited both low and high porosity values, implying that the porosity of the lithology was controlled by mechanisms besides the early weathering (Fig. 10).

Marins et al. (2022) studied core samples from five wells from the Badejo and Linguado fields (3-BD-13-RJS, 7-BD-11A-RJS, 3-BD-15C-RJS, 3-LI-04-RJS, and 7-LI-03-RJS) and observed that, in some intervals, weathering resulted in early pore filling and a reduction in porosity; this phenomenon was also observed by Mizusaki et al. (1988). Marins et al. (2022) also noted that less weathered lava flows preserved the high porosity associated with primary structures (such as vesicles and cooling fractures), which represent higher reservoir quality. They also showed how petrophysical properties varied between lava flows (volcanic intra-facies) and that the best values of porosity matrix were associated with vesicular basalts and intra-zones of rubbly pahoehoe lava bodies (Marins et al., 2022). Studies on analog onshore lava flows of the Paraná Basin had similar findings regarding primary structures in fractured, vesicular, rubbly pahoehoe lava intervals (Barreto et al., 2017; Rossetti et al., 2018).

Despite the lack of detailed data on the fracture system, the approach adopted was successful in allowing us to create a model for the estimation of the storage capacity of the basaltic formation for the purposes of fluid injection (Liu et al., 2019; Chaudhary et al., 2022; Ratouis et al., 2022). This volumetric method represents a conservative and reasonable estimate of the sequestration capacity of the hypothetical model. The estimated storage capacity of the hypothetical interval presented here highlights the feasibility of the Cabiúnas Formation for CO₂ sequestration projects. The model suggests that the CO₂ injections into the upper 300 m of the basaltic sequence in the selected zones in the Badejo Field would be capable of storing 15.8–47 Mt of CO₂ (Fig. 8). The calculation was conducted for the range of viable thicknesses associated with a specific isotropic porosity (10%, 15%, 20%) as well as two%-CO₂ dilutions (5% and 10%).

Volcanic rocks are widely distributed in the Campos and Santos basins, in both the post-salt and pre-salt intervals (Neves et al., 2019; Ren et al., 2020; Magee et al., 2021). Mineralization-based storage solution using diluted CO₂ do not require cap rocks because the CO₂ does not form a buoyant plume, and most of the CO₂ reacts with the rocks within a short period (2–3 years) (Alfredsson et al., 2013; Gislason and Oelkers, 2014; Snæbjörnsdóttir et al., 2014). Furthermore, the water needed for the CO₂ injection process will not be an issue due to the availability of seawater. Another advantage of using the Cabiúnas Formation for injection operations is the presence of overlying deposits of the Lagoa Feia

Group that can act as cap rocks (Fig. 4), which will allow also to use the option for the injection of supercritical CO₂.

In summary, the main advantages of CCS projects utilizing mineral carbonation techniques in the basaltic sequence of the Campos Basin for the sequestration of CO₂ emissions from pre-salt production are 1) the suitability of the Cabiúnas volcanic sequence for mineralization-based CO₂ sequestration; 2) the vast volumes of basaltic rocks located in the shallow water pre-salt section of Campos Basin, which reduce the cost of operation; 3) its geographic proximity to the source of the emissions; 4) its proximity existing infrastructure for the transportation of CO₂ from emission sources to future injection hubs (pipeline systems are already installed and are currently used for natural gas transportation); 5) additional sealing capabilities provided by fine-grained rocks and salt deposits positioned above the volcanic sequence, which allows the injection of supercritical CO₂ besides the diluted CO₂ option treated here.

However, this study presents some limitations regarding legacy data and assumptions made to achieve a conservative estimate of the sequestration capacity of the basaltic formation. Thus, additional work must be conducted to fully evaluate the viability of these projects, such as the sophisticated experimental and numerical modeling of factors such as their reactivity, geomechanics, the detailed definition of fluids and reservoir conditions, rock–fluid interactions during injection, and injectivity versus equivalent permeability relationship (McGrail et al., 2014; Snæbjörnsdóttir et al., 2018; Jayne et al., 2019; White et al., 2020; Xing et al., 2022).

6. Conclusions

This study presents a comprehensive evaluation of the storage capacity of the pre-salt volcanic sequence located in shallow waters of the Campos Basin for the purposes of CO₂ sequestration. We have shown that the geological sequestration of CO₂ via mineralization processes is feasible considering the regional and local characteristics of these rocks, which were previously developed as oil reservoirs. Based on the available legacy data, we evaluated the tectono-stratigraphic characteristics and thickness of the volcanic unit and conducted an updated investigation into the distribution of the porosity of the rocks by processing well log data. The study also presents a review of the main aspects that control various intrinsic reservoir parameters, such as temperature, pressure, and pH, which are essential for the future development of CO₂ injection operations. A comparison of the main boundary conditions of the reservoirs showed that they were suitable for the mineralization-based geological sequestration of CO₂. The results also showed that the tectonic control of late fluid migrations is an important mechanism that must be considered in potential injection projects. We used the hypothetical model of a 31 km² hypothetical reservoir with a thickness of 300 m based on a selected area located in the Badejo Field to estimate the storage capacity of Cabiúnas basaltic rocks, assuming a CO₂ injection into porous zones with three different porosity thresholds (10%, 15%, and 20%) and two levels of CO₂ concentration and obtained storage estimates ranging from 15.8 to 47.0 Mt. Thus, this could represent another alternative for the safe geological sequestration of CO₂ over the next few decades, especially considering the growing demand for geological storage for gasses produced by the pre-salt operations in the region. The occurrence of vast amounts of volcanic rocks in this region also represents cost-related advantages due to its potential CO₂-trapping mechanism and its geographical proximity to emission sources and pre-existing infrastructure for gas transportation in the pre-salt province. Future studies are required to address issues that were not discussed here, such as the option of injecting supercritical CO₂, equivalent permeability/injectivity relationship, geomechanics, reactive transport, and the impact of fluid characteristics of the reservoirs for carbonation techniques.

Author statement

G.M.S.R, J.A.B, and A.F.L.A conceived the idea and the potential of contribution. J.A.B, G.M.S.R and J.C.T.O. processing of the geophysical surveys and borehole data. Interpretation and modeling of seismic data. Estimate of the storage capacity. G.M.S.R and J.A.B wrote the manuscript and prepared the figures with support from A.F.L.A, O.J.C.F, C.J. B, and R.S.M. J.AB. and C.J.B discussed the results and commented on the final version of the manuscript.

Declaration of Competing Interest

The authors declare that they have no known competing financial interests or personal relationships that could have appeared to influence the work reported in this paper.

Data availability

No data was used for the research described in the article.

Acknowledgments

We thank the National Agency for Petroleum, Natural Gas, and Biofuels for providing the geological and geophysical data used in this research and the DGB Earth Sciences for academic support. JAB also thanks the grant provided by Council for Scientific and Technological Development - CNPq (315343/2020-6). We thank Professor Benjamin M. Tutolo and the anonymous reviewer for their excellent and constructive suggestions that helped significantly improve this manuscript.

References

- Alcalde, J., Flude, S., Wilkinson, M., Johnson, G., Edlmann, K., Bond, C.E., Scott, V., Gilfillan, S.M.V., Ogaya, X., Haszeldine, R.S., 2018. Estimating geological CO₂ storage security to deliver on climate mitigation. *Nat. Commun.* 9 (1), 1–13. <https://doi.org/10.1038/s41467-018-04423-1>.
- Alfredsson, H.A., Oelkers, E.H., Hardarsson, B.S., Franzson, H., Gunnlaugsson, E., Gislason, S.R., 2013. The geology and water chemistry of the Hellisheiði, SW-Iceland carbon storage site. *Int. J. Greenhouse Gas Control* 12, 399–418. <https://doi.org/10.1016/j.ijggc.2012.11.019>.
- Ali, M., Jha, N.K., Pal, N., Keshavarz, A., Hoteit, H., Sarmadivaleh, M., 2022. Recent advances in carbon dioxide geological storage, experimental procedures, influencing parameters, and future outlook. *Earth Sci. Rev.* 225, 103895 <https://doi.org/10.1016/j.earscirev.2021.103895>.
- Anderson, S.T., 2017. Risk, liability, and economic issues with long-term CO₂ storage—a review. *Nat. Resour. Res.* 26 (1), 89–112. <https://doi.org/10.1007/s11053-016-9303-6>.
- Ajayi, T., Gomes, J.S., Bera, A., 2019. A review of CO₂ storage in geological formations emphasizing modeling, monitoring and capacity estimation approaches. *Pet. Sci.* 16 (5), 1028–1063. <https://doi.org/10.1007/s12182-019-0340-8>.
- Aminu, M.D., Nabavi, S.A., Rochelle, C.A., Manovic, V., 2017. A review of developments in carbon dioxide storage. *Appl. Energy* 208, 1389–1419. <https://doi.org/10.1016/j.apenergy.2017.09.015>.
- Amonette, J.E., Johnson, T.A., Spencer, C.F., Zhong, L., Szecsody, J.E., Vermeul, V.R., 2014. Geochemical monitoring considerations for the FutureGen 2.0 project. *Energy Procedia* 63, 4095–4111. <https://doi.org/10.1016/j.egypro.2014.11.441>.
- Andrews, G. 2022. Geological Carbon Storage in Northern Irish Basalts: prospectivity and Potential. Available At SSRN: 10.2139/ssrn.4157443.
- ANP. 2019. Boletim Mensal da Produção de Petróleo e Gás Natural.
- ANP. 2021. Panorama Exploratório das Bacias de Santos e Campos: gigantes Nacionais.
- ANP. 2022. Polígono do Pré-Sal.
- Anthonsen, K.L., Aagaard, P., Bergamo, P.E.S., Gislason, S.R., Lothe, A.E., Mortensen, G. M., Snæbjörnsdóttir, S.Ó., 2014. Characterisation and selection of the most prospective CO₂ storage sites in the Nordic region. *Energy Procedia* 63, 4884–4896. <https://doi.org/10.1016/j.egypro.2014.11.519>.
- Asfahani, J., 2017. Porosity and hydraulic conductivity estimation of the basaltic aquifer in Southern Syria by using nuclear and electrical well logging techniques. *Acta Geophys.* 65 (4), 765–775. <https://doi.org/10.1007/s11600-017-0056-3>.
- Aydin, G., Karakurt, I., Aydiner, K., 2010. Evaluation of geologic storage options of CO₂: applicability, cost, storage capacity and safety. *Energy Policy* 38 (9), 5072–5080. <https://doi.org/10.1016/j.enpol.2010.04.035>.
- Bai, M., Zhang, Z., Fu, X., 2016. A review on well integrity issues for CO₂ geological storage and enhanced gas recovery. *Renew. Sustain. Energy Rev.* 59, 920–926. <https://doi.org/10.1016/j.rser.2016.01.043>.
- Barreto, C.J.S., de Lima, E.F., Goldberg, K., 2017. Primary vesicles, vesicle-rich segregation structures and recognition of primary and secondary porosities in lava flows from the Paraná igneous province, southern Brazil. *Bull. Volcanol.* 79 (4), 1–17. <https://doi.org/10.1007/s00445-017-1116-x>.
- Bataille, C., Waisman, H., Briand, Y., Svensson, J., Vogt-Schilb, A., Jaramillo, M., Delgado, R., Arguello, R., Clarke, L., Wild, T., Lallana, F., Bravo, G., Nadal, G., Le Treut, G., Godínez, G., Quiros-Tortos, J., Pereira, E., Howells, M., Buiria, D., Tovilla, J., Farbes, J., Ryan, J., Ugarte, D.D.L.T., Requejo, F., Gomez, X., Soria, R., Villamar, D., Rochedo, P., Imperio, M., 2020. Net-zero deep decarbonization pathways in Latin America: challenges and opportunities. *Energy Strategy Rev.* 30, 100510 <https://doi.org/10.1016/j.esr.2020.100510>.
- Beltrão, R.L.C., Sombra, C.L., Lage, A.C.V., Netto, J.R.F., Henriques, C.C.D., 2009. SS: pre-salt Santos basin-challenges and new technologies for the development of the pre-salt cluster, Santos basin, Brazil. Day 1 Mon. In: Proceedings of the Offshore Technology Conference. <https://doi.org/10.4043/19880-MS>. May 04 2009..
- Bérest, P., Brouard, B., 2003. Safety of salt caverns used for underground storage blow out; mechanical instability; seepage; cavern abandonment. *Oil Gas Sci. Technol.* 58 (3), 361–384. <https://doi.org/10.2516/ogst:2003023>.
- Bruhn, C.H., Gomes, J.A.T., Del Lucches Jr, C., Johann, P.R., 2003. Campos basin: reservoir characterization and management-Historical overview and future challenges. In: Proceedings of the Offshore Technology Conference. Offshore Technology Conference.
- Cao, C., Liu, H., Hou, Z., Mehmood, F., Liao, J., Feng, W., 2020. A review of CO₂ storage in view of safety and cost-effectiveness. *Energies* 13 (3), 600. <https://doi.org/10.3390/en1303060>.
- Chaudhary, M., Sharma, R., Kapoor, D., Sadiq, M., 2022. Formation evaluation of Deccan (basalt) trap basement of Kutch Offshore basin, Gulf of Kutch, India. *J. Pet. Sci. Eng.* 217, 110854 <https://doi.org/10.1016/j.petrol.2022.110854>.
- Clark, D.E., Gunnarsson, I., Aradóttir, E.S., Arnarson, M.P., Porgeirsson, P.A., Sigurðardóttir, S.S., Sigfússon, B., Snæbjörnsdóttir, S., Oelkers, E.H., Gíslason, S.R., 2018. The chemistry and potential reactivity of the CO₂-H₂S charged injected waters at the basaltic CarbFix2 site, Iceland. *Energy Procedia* 146, 121–128. <https://doi.org/10.1016/j.egypro.2018.07.016>.
- Clark, D.E., Oelkers, E.H., Gunnarsson, I., Sigfússon, B., Snæbjörnsdóttir, S.Ó., Aradóttir, E.S., Gíslason, S.R., 2020. CarbFix2: CO₂ and H₂S mineralization during 3.5 years of continuous injection into basaltic rocks at more than 250°C. *Geochim. Cosmochim. Acta* 279, 45–66. <https://doi.org/10.1016/j.gca.2020.03.039>.
- Cornelius, S., 2021. Geological sources of CO₂ in the Pre-Salt Reservoirs of Santos, Campos and Espírito Santo Basins, Brazilian SE Atlantic Margin. In: Proceedings of the 3rd HGS and EAGE Conference on Latin America, 2021. European Association of Geoscientists & Engineers, pp. 1–4. <https://doi.org/10.3997/2214-4609.202188008>.
- Costa, A.M., Costa, P.V., Miranda, A.C., Goulart, M.B., Udebhulu, O.D., Ebecken, N.F., Azevedo, R.C., de Eston, S.M., de Tomi, G., Mendes, A.B., Meneghini, J.R., Nishimoto, K., Sampaio, C.M., Brandão, C., Breda, A., 2019. Experimental salt cavern in offshore ultra-deep water and well design evaluation for CO₂ abatement. *Int. J. Min. Sci. Technol.* 29 (5), 641–656. <https://doi.org/10.1016/j.ijmst.2019.05.002>.
- d'Almeida, K.S., Vilela, P.C., Cardoso, R.A., Fernandes, R.F., Souza, M.F.F., 2018. Ocorrência de CO₂ em campos petrolíferos na margem leste brasileira. *Empresa de Pesquisa Energética*.
- Damen, K., Faaij, A., Turkenburg, W., 2006. Health, safety and environmental risks of underground CO₂ storage—overview of mechanisms and current knowledge. *Clim. Change* 74 (1), 289–318. <https://doi.org/10.1007/s10584-005-0425-9>.
- de Castro, J.C., 2006. Evolução dos conhecimentos sobre as coquinas-reservatório da Formação Lagoa Feia no trend Badejo-Linguado-Pampo, Bacia de Campos. *Geociências* 25 (2), 175–186.
- de Castro, R.D., Picolini, J.P., 2016. Main features of the Campos Basin regional geology. *Geol. Geomorphol.* 1, 1–12. <https://doi.org/10.1016/B978-85-352-8444-7.5.0008-1>.
- de Freitas, V.A., dos Santos Vital, J.C., Rodrigues, B.R., Rodrigues, R., 2022. Source rock potential, main depocenters, and CO₂ occurrence in the pre-salt section of Santos Basin, southeast Brazil. *J. South Am. Earth Sci.* 115, 103760 <https://doi.org/10.1016/j.james.2022.103760>.
- de Lima, A.L.B., da Silva, T.F., González, M.B., Peralba, M.D.C.R., Jural, P.A., Lenz, R.L., Barrionuevo, S., Dubois, D.S., Spigolon, A.L.D., 2022. Characterization of heavy oils from the Campos Basin, Brazil: free biomarkers in oils, adsorbed and occluded in asphaltene structures. *J. Pet. Sci. Eng.* 215, 110542 <https://doi.org/10.1016/j.jpse.2022.110542>.
- Dinescu, S., Radu, S.M., Florea, A., Danciu, C., Tomuș, O.B., Popescu, S., 2021. Possible Risks of CO₂ Storage in Underground Salt Caverns. *Ann. Univ. Petroşani* 23, 27–36.
- Drexler, S., Correia, E.L., Jerdy, A.C., Cavadas, L.A., Couto, P., 2019. Effect of CO₂ injection on the interfacial tension for a Brazilian Pre-Salt field. In: Proceedings of the Offshore Technology Conference Brasil. OnePetro. <https://doi.org/10.4043/29769-MS>.
- EPE, 2020. Estudo sobre o aproveitamento do gás natural do pré-sal.
- EPE, 2021. Brazilian oil and gas report 2020/2021.
- Fawad, M., Mondol, N.H., 2022. Monitoring geological storage of CO₂ using a new rock physics model. *Sci. Rep.* 12 (1), 1–11. <https://doi.org/10.1038/s41598-021-04400-7>.
- Fox, L.M., . 2022. Stratigraphic and Geochemical Evaluation of Distal Flows of the Columbia River Flood Basalts in the Greater Vale Area, Southeastern Oregon.
- Friedmann, S.J., Dooley, J.J., Held, H., Edenhofer, O., 2006. The low cost of geological assessment for underground CO₂ storage: policy and economic implications. *Energy Convers. Manage.* 47 (13–14), 1894–1901. <https://doi.org/10.1016/j.enconman.2005.09.006>.

- Fuss, S., Canadell, J.G., Ciais, P., Jackson, R.B., Jones, C.D., Lyngfelt, A., Peters, G.P., Van Vuuren, D.P., 2020. Moving toward net-zero emissions requires new alliances for carbon dioxide removal. *One Earth* 3 (2), 145–149. <https://doi.org/10.1016/j.oneear.2020.08.002>.
- Gadikota, G., 2021. Carbon mineralization pathways for carbon capture, storage and utilization. *Commun. Chem.* 4 (1), 23.
- Gamboa, L., Ferraz, A., Baptista, R., Neto, E.V.S., 2019. Geotectonic controls on CO₂ formation and distribution processes in the Brazilian pre-salt basins. *Geosciences* 9 (6), 252. <https://doi.org/10.3390/geosciences9060252> (Basel).
- Gholami, R., Raza, A., Iglauser, S., 2021. Leakage risk assessment of a CO₂ storage site: a review. *Earth Sci. Rev.* 223, 103849 <https://doi.org/10.1016/j.earscirev.2021.103849>.
- Gislason, S.R., Wolff-Boenisch, D., Stefansson, A., Oelkers, E.H., Gunnlaugsson, E., Sigurdardottir, H., Sigfusson, B., Broecker, W.S., Matter, J.M., Martin, S., Gudni, A., Fridriksson, T., 2010. Mineral sequestration of carbon dioxide in basalt: a pre-injection overview of the CarbFix project. *Int. J. Greenhouse Gas Control* 4 (3), 537–545. <https://doi.org/10.1016/j.ijggc.2009.11.013>.
- Gislason, S.R., Broecker, W.S., Gunnlaugsson, E., Snæbjörnsdóttir, S., Mesfin, K.G., Alfredsson, H.A., Aradóttir, E.S., Sigfusson, B., Gunnarsson, I., Stute, M., Matter, J.M., Arnarson, M.Th., Galeczka, I.M., Gudbrandsson, S., Stockman, G., Wolff-Boenisch, D., Stefansson, A., Ragnheiðardóttir, E., Flathen, T., Gysi, A.P., Olssen, J., Didriksen, K., Stipp, S., Menez, B., Oelkers, E.H., 2014. Rapid solubility and mineral storage of CO₂ in basalt. *Energy Procedia* 63, 4561–4574. <https://doi.org/10.1016/j.egypro.2014.11.489>.
- Gislason, S.R., Oelkers, E.H., 2014. Carbon storage in basalt. *Science* 344 (6182), 373–374. <https://doi.org/10.1126/science.1250828>.
- Gislason, S.R., Sigurdardóttir, H., Aradóttir, E.S., Oelkers, E.H., 2018. A brief history of CarbFix: challenges and victories of the project's pilot phase. *Energy Procedia* 146, 103–114. <https://doi.org/10.1016/j.egypro.2018.07.014>.
- Godoi, J.M.A., dos Santos Matai, P.H.L., 2021. Enhanced oil recovery with carbon dioxide geosequestration: first steps at Pre-salt in Brazil. *J. Pet. Explor. Prod.* 11 (3), 1429–1441. <https://doi.org/10.1007/s13202-021-01102-8>.
- Goulart, M.B.R., da Costa, P.V.M., da Costa, A.M., Miranda, A.C., Mendes, A.B., Ebecken, N.F., Meneghini, J.R., Nishimoto, K., Assi, G.R., 2020. Technology readiness assessment of ultra-deep salt caverns for carbon capture and storage in Brazil. *Int. J. Greenhouse Gas Control* 99, 103083. <https://doi.org/10.1016/j.ijggc.2020.103083>.
- Grusson, Y., Sun, X., Gascoin, S., Sauvage, S., Raghavan, S., Anctil, F., Sánchez-Pérez, J.M., 2015. Assessing the capability of the SWAT model to simulate snow, snow melt and streamflow dynamics over an alpine watershed. *J. Hydrol.* 531, 574–588. <https://doi.org/10.1016/j.jhydrol.2015.10.070> (Amst).
- Guardado, L.R., Gamboa, L.A.P., Lucchesi, C.F., 1990. Petroleum geology of the Campos Basin, Brazil, a model for a producing Atlantic type basin. Divergent/pассив Margin Basins.
- Guardado, L.R., Spadini, A.R., Brandão, J.S.L., Mello, M.R., 2000. Petroleum System of the Campos Basin, Brazil. *AAPG Memoir* 73, 317–324. Chapter 22.
- Gunnarsson, I., Aradóttir, E.S., Oelkers, E.H., Clark, D.E., Arnarson, M.B., Sigfusson, B., Snæbjörnsdóttir, S., Matter, J.M., Stute, M., Júlfusson, B.M., Gislason, S.R., 2018. The rapid and cost-effective capture and subsurface mineral storage of carbon and sulfur at the CarbFix 2 site. *Int. J. Greenhouse Gas Control* 79, 117–126. <https://doi.org/10.1016/j.ijggc.2018.08.014>.
- Gupta, S.D., Chatterjee, R., Farooqui, M.Y., 2012. Formation evaluation of fractured basement, Cambay Basin, India. *J. Geophys. Eng.* 9 (2), 162–175. <https://doi.org/10.1088/1742-2132/9/2/162>.
- He, H., Li, S., Liu, C., Kong, C., Jiang, Q., Chang, T., 2020. Characteristics and quantitative evaluation of volcanic effective reservoirs: a case study from Junggar Basin, China. *J. Pet. Sci. Eng.* 195, 107723 <https://doi.org/10.1016/j.petrol.2020.107723>.
- Hong, S., Moon, S., Cho, J., Park, A.H.A., Park, Y., 2022. Effects of Mg ions on the structural transformation of calcium carbonate and their implication for the tailor-synthesized carbon mineralization process. *J. CO₂ Util.* 60, 101999 <https://doi.org/10.1016/j.jcou.2022.101999>.
- Jayne, R.S., Wu, H., Polley, R.M., 2019. A probabilistic assessment of geomechanical reservoir integrity during CO₂ sequestration in flood basalt formations. *Greenhouse Gases Sci. Technol.* 9 (5), 979–998. <https://doi.org/10.1002/ghg.1914>.
- Kelemen, P.B., McQueen, N., Wilcox, J., Renforth, P., Dipple, G., Vänekeuren, A.P., 2020. Engineered carbon mineralization in ultramafic rocks for CO₂ removal from air: review and new insights. *Chem. Geol.* 550, 119628 <https://doi.org/10.1016/j.chemgeo.2020.119628>.
- Kelemen, P., Benson, S.M., Pilorgé, H., Psarras, P., Wilcox, J., 2019. An overview of the status and challenges of CO₂ storage in minerals and geological formations. *Front. Clim.* 1 (9) <https://doi.org/10.3389/fclim.2019.00009>.
- Koukouzas, N., Koutsovitis, P., Tyrologou, P., Karkalis, C., Arvanitis, A., 2019. Potential for mineral carbonation of CO₂ in Pleistocene basaltic rocks in Volos region (central Greece). *Minerals*, 9 (10), 627. <https://doi.org/10.3390/min9100627>.
- Lamur, A., Kendrick, J.E., Eggertsson, G.H., Wall, R.J., Ashworth, J.D., Lavallée, Y., 2017. The permeability of fractured rocks in pressurized volcanic and geothermal systems. *Sci. Rep.* 7 (1), 1–9. <https://doi.org/10.1038/s41598-017-05460-4>.
- Larkin, P., Gracie, R., Shafeei, A., Dusseault, M., Sarkarfarshi, M., Aspinall, W., Krewski, D., 2019. Uncertainty in risk issues for carbon capture and geological storage: findings from a structured expert elicitation. *10.1504/IJRAM.2019.103335*.
- Lavalleur, H.J., Colwell, F.S., 2013. Microbial characterization of basalt formation waters targeted for geological carbon sequestration. *FEMS Microbiol. Ecol.* 85 (1), 62–73. <https://doi.org/10.1111/1574-6941.12098>.
- Leung, D.Y., Caramanna, G., Maroto-Valer, M.M., 2014. An overview of current status of carbon dioxide capture and storage technologies. *Renew. Sustain. Energy Rev.* 39, 426–443. <https://doi.org/10.1016/j.rser.2014.07.093>.
- Lima, R.O., de L Cunha, A., Santos, J.A.O., Garcia, A.J.V., dos Santos, J.P.L., 2020. Assessment of continuous and alternating CO₂ injection under Brazilian-pre-salt-like conditions. *J. Pet. Explor. Prod. Technol.* 10 (7), 2947–2956. <https://doi.org/10.1007/s13202-020-00968-4>.
- Liu, D., Agarwal, R., Li, Y., Yang, S., 2019. Reactive transport modeling of mineral carbonation in unaltered and altered basalts during CO₂ sequestration. *Int. J. Greenhouse Gas Control* 85, 109–120. <https://doi.org/10.1016/j.ijggc.2019.04.006>.
- Lobo, J.T., Duarte, B.P., Szatmari, P., de Castro Valente, S., 2007. Basaltos continentais do Cretáceo Inferior da bacia de Campos, SE do Brasil: compilação de dados e petrógenese. *Braz. J. Geol.* 37 (2), 224–236.
- Luhmann, A.J., Tutolo, B.M., Bagley, B.C., Mildner, D.F., Seyfried Jr, W.E., Saar, M.O., 2017. Permeability, porosity, and mineral surface area changes in basalt cores induced by reactive transport of CO₂-rich brine. *Water Resour. Res.* 53 (3), 1908–1927. <https://doi.org/10.1002/2016WR019216>.
- Macente, A., Vanorio, T., Miller, K.J., Fusseis, F., Butler, I.B., 2019. Dynamic evolution of permeability in response to chemo-mechanical compaction. *J. Geophys. Res. Solid Earth* 124 (11), 11204–11217. <https://doi.org/10.1029/2019JB017750>.
- Magee, C., Pichel, L.M., Madden-Nadeau, A.L., Jackson, C.A.L., Mohriak, W., 2021. Salt–magma interactions influence intrusion distribution and salt tectonics in the Santos Basin, offshore Brazil. *Basin Res.* 33 (3), 1820–1843. <https://doi.org/10.1111/bre.12537>.
- Marieni, C., Voigt, M., Clark, D.E., Gislason, S.R., Oelkers, E.H., 2021. Mineralization potential of water-dissolved CO₂ and H₂S injected into basalts as function of temperature: freshwater versus Seawater. *Int. J. Greenhouse Gas Control* 109, 103357. <https://doi.org/10.1016/j.ijggc.2021.103357>.
- Marins, G.M., Parizek-Silva, Y., Millett, J.M., Jerram, D.A., Rossetti, L.M., e Souza, A.D. J., Planke, S., Bevilacqua, L.A., Carmo, I.D.O., 2022. Characterization of volcanic reservoirs; insights from the Badejo and Linguado oil field, Campos Basin, Brazil. *Mar. Pet. Geol.*, 105950 <https://doi.org/10.1016/j.marpetgeo.2022.105950>.
- Martin-Roberts, E., Scott, V., Flude, S., Johnson, G., Haszeldine, R.S., Gilfillan, S., 2021. Carbon capture and storage at the end of a lost decade. *One Earth* 4 (11), 1569–1584. <https://doi.org/10.1016/j.oneear.2021.10.002>.
- Matias, H.C., Ninci, B., Guangsheng, X., Pessoa, M.C., Mattos, F., Margem, R., Carballo, J., Esteban, M., Tritlla, R., Loma, R., Pimentel, G., 2015. Unlocking Pandora-Insights from Pre-salt Reservoirs in Campos and Santos Basins (Offshore Brazil). In: Proceedings of the 77th EAGE Conference and Exhibition 2015, 2015. European Association of Geoscientists & Engineers, pp. 1–5. <https://doi.org/10.3997/2214-4609.201412891>.
- Matter, J.M., Stute, M., Hall, J., Mesfin, K., Snæbjörnsdóttir, S.Ó., Gislason, S.R., Oelkers, E.H., Sigfusson, B., Gunnarsson, I., Aradóttir, E.S., Alfredsson, H.A., Gunnlaugsson, E., Broecker, W.S., 2014. Monitoring permanent CO₂ storage by in situ mineral carbonation using a reactive tracer technique. *Energy Procedia* 63, 4180–4185. <https://doi.org/10.1016/j.egypro.2014.11.450>.
- McGrail, B.P., Schaeff, H.T., Ho, A.M., Chien, Y.J., Dooley, J.J., Davidson, C.L., 2006. Potential for carbon dioxide sequestration in flood basalts. *J. Geophys. Res. Solid Earth* 111 (B12). <https://doi.org/10.1029/2005JB004169>.
- McGrail, B.P., Spane, F.A., Amontone, J.E., Thompson, C.R., Brown, C.F., 2014. Injection and monitoring and monitoring at the Wallula basalt pilot project. *Energy Procedia* 63, 2939–2948. <https://doi.org/10.1016/j.egypro.2014.11.316>.
- McGrail, B.P., Schaeff, H.T., Spane, F.A., Horner, J.A., Owen, A.T., Cliff, J.B., Qafoku, O., Thompson, C.J., Sullivan, E.C., 2017. Wallula basalt pilot demonstration project: post-injection results and conclusions. *Energy Procedia* 114, 5783–5790. <https://doi.org/10.1016/j.egypro.2017.03.1716>.
- Mechler, E., Brown, S., Fennell, P.S., Mac Dowell, N., 2017. CO₂ capture and storage (CCS) cost reduction via infrastructure right-sizing. *Chem. Eng. Res. Des.* 119, 130–139. <https://doi.org/10.1016/j.cherd.2017.01.016>.
- Milani, E.J., Thomaz Filho, A., 2000. Sedimentary basins of south America. *Tectonic Evol. South Am.* 31, 389–449.
- Mizuno, T.A., Mizusaki, A.M.P., Lykawka, R., 2018. Facies and paleoenvironments of the Coqueiros Formation (Lower Cretaceous, Campos Basin): a high frequency stratigraphic model to support pre-salt "coquinas" reservoir development in the Brazilian continental margin. *J. South Am. Earth Sci.* 88, 107–117. <https://doi.org/10.1016/j.jsames.2018.07.007>.
- Mizusaki, A.M.P., Filho, A.T., Valença, J., 1988. Volcano sedimentary sequence of neocomian age in Campos Basin (Brazil). *Rev. Bras. Geociências*, 18 (3), 247–251.
- Mizusaki, A.M.P., 1986. Rochas igneo-básicas do neocomiano da Bacia de Campos: caracterização e comportamento como reservatório de hidrocarbonetos. *Anuário do Instituto de Geociências* 16, 77–78.
- Moghlanloo, R.G., Yan, X., Law, G., Roshani, S., Babb, G., Herron, W., 2017. Challenges associated with CO₂ sequestration and hydrocarbon recovery. In: Recent Advances in Carbon Capture and Storage. pp. 209.
- Mohriak, W.U., Mello, M.R., Dewey, J.F., Maxwell, J.R., 1990. Petroleum geology of the Campos Basin, offshore Brazil. *Geol. Soc.* 50 (1), 119–141. <https://doi.org/10.1144/GSL.SP.1990.050.01.07>.
- Navarro, J., Teramoto, E.H., Engelbrecht, B.Z., Kiang, C.H., 2020. Assessing hydrofacies and hydraulic properties of basaltic aquifers derived from geophysical logging. *Braz. J. Geol.* 50 (04) <https://doi.org/10.1590/2317-48892020200013>.
- Neves, I.D.A., Lupinacci, W.M., Ferreira, D.J.A., Zambrini, J.P.R., Oliveira, L.O.A., Azul, M.O., Ferrari, A.L., Gamboa, L.A.P., 2019. Presalt reservoirs of the Santos Basin: cyclicity, electrofacies, and tectonic-sedimentary evolution. *Interpretation* 7 (4), SH33–SH43. <https://doi.org/10.1190/INT-2018-0237.1>.
- Ning, L., Dexing, Q., Qingfeng, L., Hongliang, W., Youshen, F., Lixin, D., Qingfu, F., Kewen, W., 2009. Theory on logging interpretation of igneous rocks and its

- application. Pet. Explor. Dev. 36 (6), 683–692. [https://doi.org/10.1016/S1876-3804\(10\)60002-X](https://doi.org/10.1016/S1876-3804(10)60002-X).
- Oreiro, S.G., 2006. Interpretação sísmica dos eventos magmáticos pós-aptianos no Alto de Cabo Frio, sudeste do Brasil, gênese e relação com os lineamentos pré-Sal. <http://www.bdtd.uerj.br/handle/1/7000>.
- Pawar, R.J., Bromhal, G.S., Carey, J.W., Foxall, W., Korre, A., Ringrose, P.S., Tucker, O., Watson, M.N., White, J.A., 2015. Recent advances in risk assessment and risk management of geologic CO₂ storage. Int. J. Greenhouse Gas Control 40, 292–311. <https://doi.org/10.1016/j.ijgac.2015.06.014>.
- Pereira, P., Ribeiro, C., Carneiro, J., 2021. Identification and characterization of geological formations with CO₂ storage potential in Portugal. Pet. Geosci. 27 (3) <https://doi.org/10.1144/petgeo2020-123>.
- Pogge von Strandmann, P.A., Burton, K.W., Snæbjörnsdóttir, S.O., Sigfusson, B., Aradóttir, E.S., Gunnarsson, I., Alfredsson, H.A., Mesfin, K.G., Oelkers, E.H., Gislason, S.R., 2019. Rapid CO₂ mineralisation into calcite at the CarbFix storage site quantified using calcium isotopes. Nat. Commun. 10 (1), 1–7. <https://doi.org/10.1038/s41467-019-10003-8>.
- Ratouis, T.M., Snæbjörnsdóttir, S.Ó., Voigt, M.J., Sigfusson, B., Gunnarsson, G., Aradóttir, E.S., Hjörleifsdóttir, V., 2022. CarbFix2: a transport model of long-term CO₂ and H₂S injection into basaltic rocks at Hellisheiði, SW-Iceland. Int. J. Greenhouse Gas Control 114, 103586. <https://doi.org/10.1016/j.ijgac.2022.103586>.
- Raza, A., Glatz, G., Gholami, R., Mahmoud, M., Alafnan, S., 2022. Carbon mineralization and geological storage of CO₂ in basalt: mechanisms and technical challenges. Earth Sci. Rev. 229, 104036 <https://doi.org/10.1016/j.earscrev.2022.104036>.
- Reis, G.D.S., 2013. A formação Serra Geral (cretáceo, bacia do Paraná) como análogo para os reservatórios ígneos-básicos da margem continental brasileira. <http://hdl.handle.net/10183/72233>.
- Ren, K., Zhao, J., Liu, Q., Zhao, J., 2020. Hydrocarbons in igneous rock of Brazil: a review. Pet. Res. 5 (3), 265–275. <https://doi.org/10.1016/j.ptlrs.2020.06.001>.
- Rockett, G.C., Ketzer, J.M.M., Ramírez, A., Van den Broek, M., 2013. CO₂ storage capacity of Campos Basin's oil fields, Brazil. Energy Procedia 37, 5124–5133. <https://doi.org/10.1016/j.egypro.2013.06.427>.
- Rosa, M.C., Vincenzielli, M.G.C., 2017. Seismic Attribute Analysis in carbonate reservoir physical properties distribution: neobarremian-Eoaptian coquina reservoir case. In: Proceedings of the 15th International Congress of the Brazilian Geophysical Society & EXPOGEF. Brazilian Geophysical Society, pp. 270–273. <https://doi.org/10.1190/sbsf2017-053>. Rio de Janeiro, Brazil, 31 July–3 August 2017.
- Rossetti, L., Lima, E.F., Waichel, B.L., Hole, M.J., Simões, M.S., Scherer, C.M., 2018. Lithostratigraphy and volcanology of the Serra Geral Group, Paraná-Etendeka Igneous Province in Southern Brazil: towards a formal stratigraphical framework. J. Volcanol. Geotherm. Res. 355, 98–114. <https://doi.org/10.1016/j.jvolgeores.2017.05.008>.
- Rubin, E.S., Davison, J.E., Herzog, H.J., 2015. The cost of CO₂ capture and storage. Int. J. Greenhouse Gas Control 40, 378–400. <https://doi.org/10.1016/j.ijgac.2015.05.018>.
- Rubin, E.S., Short, C., Booras, G., Davison, J., Ekstrom, C., Matuszewski, M., McCoy, S., 2013. A proposed methodology for CO₂ capture and storage cost estimates. Int. J. Greenhouse Gas Control 17, 488–503. <https://doi.org/10.1016/j.ijgac.2013.06.004>.
- Sampaio, M.A., de Mello, S.F., Schiozzer, D.J., 2020. Impact of physical phenomena and cyclical reinjection in miscible CO₂-WAG recovery in carbonate reservoirs. J. Pet. Explor. Prod. Technol. 10 (8), 3865–3881. <https://doi.org/10.1007/s13202-020-00925-1>.
- Santos Neto, E.V., Cerqueira, J.R., Prinzhofe, A., 2012. Origin of CO₂ in Brazilian basins. Search Discovery Article 40969.
- Schmelz, W.J., Hochman, G., Miller, K.G., 2020. Total cost of carbon capture and storage implemented at a regional scale: northeastern and midwestern United States. Interface Focus 10 (5), 20190065. <https://doi.org/10.1098/rsfs.2019.0065>.
- Schwartz, M.O., 2018. The new Wallula CO₂ project may revive the old Columbia River Basalt (western USA) nuclear-waste repository project. Hydrogeol. J. 26 (1), 3–6. <https://doi.org/10.1007/s10040-017-1632-y>.
- S&P Global, 2021. CCUS in the decarbonization of upstream production in Brazil. <https://www.spglobal.com/commodityinsights/en/ci/research-analysis/ccus-in-the-decarbonization-of-upstream-production-in-brazil.html> (Accessed 27 December 2022).
- Slagle, A.L., Goldberg, D.S., 2011. Evaluation of ocean crustal Sites 1256 and 504 for long-term CO₂ sequestration. Geophys. Res. Lett. 38 (16) <https://doi.org/10.1029/2011GL048613>.
- Smith, E., Morris, J., Kheshgi, H., Teletzke, G., Herzog, H., Paltsev, S., 2021. The cost of CO₂ transport and storage in global integrated assessment modeling. Int. J. Greenhouse Gas Control 109, 103367. <https://doi.org/10.1016/j.ijgac.2021.103367>.
- Snæbjörnsdóttir, S.Ó., Wiese, F., Fridriksson, T., Ármannsson, H., Einarsson, G.M., Gislason, S.R., 2014. CO₂ storage potential of basaltic rocks in Iceland and the oceanic ridges. Energy Procedia 63, 4585–4600. <https://doi.org/10.1016/j.egypro.2014.11.491>.
- Snæbjörnsdóttir, S.Ó., Gislason, S.R., Galeczka, I.M., Oelkers, E.H., 2018. Reaction path modelling of in-situ mineralisation of CO₂ at the CarbFix site at Hellisheiði, SW-Iceland. Geochim. Cosmochim. Acta 220, 348–366. <https://doi.org/10.1016/j.gca.2017.09.053>.
- Snæbjörnsdóttir, S.Ó., Sigfusson, B., Marieni, C., Goldberg, D., Gislason, S.R., Oelkers, E. H., 2020. Carbon dioxide storage through mineral carbonation. Nat. Rev. Earth Environ. 1 (2), 90–102. <https://doi.org/10.1038/s43017-019-0011-8>.
- Span, R., Wagner, W., 1996. A new equation of state for carbon dioxide covering the fluid region from the triple-point temperature to 1100K at pressures up to 800MPa. J. Phys. Chem. Ref. Data 25 (6), 1509–1596. <https://doi.org/10.1063/1.555991>.
- Stenhouse, M.J., Gale, J., Zhou, W., 2009. Current status of risk assessment and regulatory frameworks for geological CO₂ storage. Energy Procedia 1 (1), 2455–2462. <https://doi.org/10.1016/j.egypro.2009.02.007>.
- Stica, J.M., Zalán, P.V., Ferrari, A.L., 2014. The evolution of rifting on the volcanic margin of the Pelotas Basin and the contextualization of the Paraná-Etendeka LIP in the separation of Gondwana in the South Atlantic. Mar. Pet. Geol. 50, 1–21. <https://doi.org/10.1016/j.marpetgeo.2013.10.015>.
- Takagi, M., Koide, K., Shimizu, J., Iwamoto, C., Ohoka, M., Ikeda, S., Azuma, H., 2013. Cost estimates for the CO₂ geological storage in deep saline aquifers offshore Japan: a case study. Energy Procedia 37, 3374–3378. <https://doi.org/10.1016/j.egypro.2013.06.225>.
- Tang, H., Tian, Z., Gao, Y., Dai, X., 2022. Review of volcanic reservoir geology in China. Earth Sci. Rev., 104158.
- Tutolo, B.M., Awolayo, A., Brown, C., 2021. Alkalinity generation constraints on basalt carbonation for carbon dioxide removal at the gigaton-per-year scale. Environmental. Sci. Technol. 55 (17), 11906–11915. <https://doi.org/10.1021/acs.est.1c02733>.
- Viglio, J.E., Giulio, G., Di, M., Ferreira, L.D.C., 2017. Not all glitters in the black gold: uncertainties and environmental threats of the Brazilian pre-salt. Ambiente Soc. 20, 21–38. <https://doi.org/10.1059/1809-4422ASOC58R3V2032017>.
- Villarrasa, V., 2014. Impact of CO₂ injection through horizontal and vertical wells on the caprock mechanical stability. Int. J. Rock Mech. Min. Sci. 66, 151–159. <https://doi.org/10.1016/j.ijrmms.2014.01.001>.
- Villarrasa, V., Carrera, J., 2015. Geologic carbon storage is unlikely to trigger large earthquakes and reactivate faults through which CO₂ could leak. Proc. Natl. Acad. Sci. 112 (19), 5938–5943. <https://doi.org/10.1073/pnas.1413284112>.
- Wang, Y., Yang, R., Song, M., Lenhardt, N., Wang, X., Zhang, X., Yang, S., Wang, J., Cao, H., 2018. Characteristics, controls and geological models of hydrocarbon accumulation in the Carboniferous volcanic reservoirs of the Chunfeng Oilfield, Junggar Basin, Northwestern China. Mar. Pet. Geol. 94, 65–79. <https://doi.org/10.1016/j.marpetgeo.2018.04.001>.
- Warren, J.K., 2017. Salt usually seals, but sometimes leaks: implications for mine and cavern stabilities in the short and long term. Earth Sci. Rev. 165, 302–341. <https://doi.org/10.1016/j.earscrev.2016.11.008>.
- White, S.K., Spane, F.A., Schaeff, H.T., Miller, Q.R., White, M.D., Horner, J.A., McGrail, B. P., 2020. Quantification of CO₂ mineralization at the Wallula basalt pilot project. Environ. Sci. Technol. 54 (22), 14609–14616. <https://doi.org/10.1021/acs.est.0c05142>.
- Xing, T., Zhu, W., Fusseis, F., Lisabeth, H., 2018. Generating porosity during olivine carbonation via dissolution channels and expansion cracks. Solid Earth 9 (4), 879–896. <https://doi.org/10.5194/se-9-879-2018>.
- Xing, T., Ghaffari, H.O., Mok, U., Pec, M., 2022. Creep of CarbFix basalt: influence of rock-fluid interaction. Solid Earth 13 (1), 137–160. <https://doi.org/10.5194/se-13-137-2022>.
- Zahasky, C., Thomas, D., Matter, J., Maher, K., Benson, S.M., 2018. Multimodal imaging and stochastic percolation simulation for improved quantification of effective porosity and surface area in vesicular basalt. Adv. Water Resour. 121, 235–244. <https://doi.org/10.1016/j.advwatres.2018.08.009>.
- Zakharov, N.V., Goldberg, D.S., Sullivan, E.C., Herron, M.M., Grau, J.A., 2012. Petrophysical and geochemical properties of Columbia River flood basalt: implications for carbon sequestration. Geochem. Geophys. Geosyst. 13 (11) <https://doi.org/10.1029/2012GC004305>.
- Zappone, A., Rinaldi, A.P., Grab, M., Wenning, Q.C., Roques, C., Madonna, C., Obermann, A.C., Bernasconi, S.M., Brennwald, M.S., Kipfer, R., Soom, F., Cook, P., Guglielmi, Y., Nussbaum, C., Giardini, D., Mazzotti, M., Wiemer, S., 2021. Fault sealing and caprock integrity for CO₂ storage: an in situ injection experiment. Solid Earth 12, 319–343. <https://doi.org/10.5194/se-12-319-2021>.